THE ASTRONOMICAL JOURNAL, 119:1405–1423, 2000 March

ANALYSES OF THE CURRENTLY NONECLIPSING BINARY SS LACERTAE OR SS LACERTAE'S ECLIPSES[1]

E. F. MILONE[2]
Physics and Astronomy Department, University of Calgary, Calgary T2N 1N4, AB, Canada; milone@acs.ucalgary.ca
S. J. SCHILLER[2]
Physics Department, South Dakota State University, Box 2219, Brookings, SD 57007-0395; schilles@mg.sdstate.edu
U. MUNARI
Osservatorio Astronomico di Padova, Sede di Asiago, I-36012 Asiago (VI), Italy; munari@astras.pd.astro.it
AND
J. KALLRATH
BASF-AG, ZOI/ZC-C13, D-67056 Ludwigshafen, Germany; and Department of Astronomy, University of Florida, Gainesville, FL 32611; kallrath@zx.basf-ag.de, kallrath@astro.ufl.edu
Received 1999 August 23; accepted 1999 November 18

ABSTRACT

Confirmatory evidence for changing light-curve amplitude of the former eclipsing and current SB2 system SS Lac in the Open Cluster NGC 7209 has been uncovered. Remeasured Harvard plate data and published and compiled data sets reveal that the depth of the primary minimum increased between the 1890s and 1902 and decreased in the 1920s and 1930s. A parabolic fitting of the amplitude with phase predicts a maximum at 1911.5, with an eclipse onset at 1885.3 and eclipse cessation at 1937.8. We confirm the finding of Lehmann, that the system's inclination varies with time and that a central eclipse occurred $\sim$1912, and we concur with Mossakovskaya that eclipses effectively ceased $\sim$1940. Estimates of SS Lac on plates taken at Tashkent between 1937 and 1940 further serve to confirm the result. Thus, SS Lac belongs to a small but elite class of triple systems in which changes due to dynamical effects can be seen over a single human lifetime. In order to explore the properties of the SS Lac system, recent radial velocity curves and archival photographic and visual light curves have been analyzed with versions of the Wilson-Devinney code, augmented with a simplex routine to test solution uniqueness. The modeling solutions for the Dugan-Wright light curves ostensibly indicate that the former eclipsing system is composed of two early A stars of only slightly differing masses (2.57 ± 0.16 and 2.59 ± 0.19 $M_\odot$) and effective surface temperatures (8750 ± 300 [assumed for component 1] and 8542 ± 309 K), but significantly different radii (2.38 ± 0.02 and 3.63 ± 0.07 $R_\odot$) and luminosities (30 ± 4 and 63 ± 9 $L_\odot$) for the hotter and cooler components, respectively. The light-curve solutions are compromised somewhat by variable eclipse depths over the ranges of dates of the data sets. This is especially true of the most complete light curve, that of Dugan & Wright; the others also suffer from incompleteness (that of Wachmann) and high scatter (that of Kordylewski, Pagaczewski, & Szafraniec). As a consequence, small, temporal variations in such system properties as the eccentricity, argument of periastron, modified Roche potentials, luminosities, and third light level, cannot be ruled out from currently available data. However, solutions with WD95, a self-iterating, damped–least squares version of the Wilson-Devinney program, reveal optimized inclinations for the data sets that project an inclination variation of $0\overset{\circ}{.}16\ \mathrm{yr}^{-1}$, but no evidence of apsidal motion. We find a distance for the system of 898 ± 95 pc, consistent with the value of Vansevičius et al. of 1040 ± 10 pc, and finally, on the bases of location on the sky, proper motion, radial velocity, photometry, and properties deduced in the present study, we confirm its membership in the cluster NGC 7209.

Key words: binaries: eclipsing — binaries: spectroscopic — star clusters: individual (NGC 7209) — stars: individual (SS Lacertae)

1. INTRODUCTION

The discovery of variability of SS Lacertae (BD+45°3782) is attributed to Henrietta Leavitt by Pickering (1907). Shapley & Swope (1938) state that the light-curve analysis presented by Dugan & Wright (1935) is "based on Miss Wright's measures on Harvard photographs." The first light curve, based on visual estimates, was published by Hoffmeister (1921) and subsequent photographic light curves were reported by Dugan & Wright (1935) and by Wachmann (1935, 1936). Another set of potentially usable light curves is given by Kordylewski, Pagaczewski, & Szafraniec (1961). Hoffmeister derived a very short period for the system, 1.201499 days, and a sinusoidal term for the ephemeris. The subsequent work by Dugan & Wright (1935) revealed a period of 14.41629 days, a result confirmed by Wachmann (1936).

The system was observed photometrically and spectroscopically in the early 1980s by S. J. S. as part of his Ph.D. thesis work on binaries in clusters, supplemented by additional photoelectric observations at the Rothney Astrophysical Observatory (RAO) in the interval 1989–1991. The system was a strong candidate for membership in the open cluster NGC 7209 and thus for the binaries-in-clusters

[1] Publications of the Rothney Astrophysical Observatory, No. 73.
[2] Visiting Astronomer, Dominion Astrophysical Observatory.

program at the University of Calgary. Cluster membership was suggested by several factors: proximity on the sky, proper motions, and radial velocity studies. Artiukhina (1961), Lavdovska (1962), van Schewick (1966), and Platais (1991) all identify SS Lac as a probable member on the basis of proper motions. As we note later, radial velocities also support membership. Finally, the variable lies near the blue turnoff of the cluster color-magnitude diagram (Hoag et al. 1961) where SS Lac is identified as star 4. The latter circumstance indicated SS Lac to be a suitable candidate to yield cluster turnoff masses and the evolutionary states of the components.

Although SS Lac has been included often in lists of apsidal motion candidates, no firm evidence for apsidal motion in this system has been found (Dugan & Wright 1937) other than the suspicion that it could be present because of a slight orbital eccentricity. Given the absence of such motion over a 45 yr interval, Shapley & Swope (1938) suggested that the apsidal period was probably "tens of thousands of years."

The S. J. S. photoelectric photometry of 1981 and 1982 (at RAO), in 1982–1983 (at McDonald and Table Mountain Observatories), and in the years 1989–1991 (at RAO), revealed no sign of an eclipse. Negative results have been reported also by Zakirov & Azimov (1990), Schiller et al. (1991), Schiller & Milone (1996), and Mossakovskaya (1993).

From photographic archive examination, Mossakovskaya (1993) concluded that the cessation of eclipses in SS Lac had occurred between the mid-1930s and the 1940s, although a limit in the 1950s was suggested initially by Zakirov & Azimov (1990). Lehmann (1991) suggested that the eclipses became progressively shallower prior to cessation. In the present paper, we examine this hypothesis and present evidence that strengthens his conclusion.

The presence of a binary with at least one variable orbital property in an open cluster raises the possibility of an encounter with another cluster member. The probability for such an encounter is low but certainly not zero. Consequently, the possibility of dynamical interaction makes it of interest to understand better the properties of the system and individual stars involved and to investigate such variable eclipse conditions as the dates of eclipse onset and cessation. These were the purposes of the present study. Spectroscopic observations were obtained by S. J. S. for radial velocity analysis in the mid-1980s. In these spectra, no strong evidence of duplicity could be discerned either in or outside of the Balmer lines, which strongly dominate the spectrum. Most recently, however, Tomasella & Munari (1998) have been successful in detecting the lines of both components in higher signal-to-noise ratio (S/N) and higher resolution echelle spectra from Asiago. In their study, only the Balmer lines Hα, Hβ, and Hγ were used to determine radial velocities. Tomasella & Munari (1998) analyzed their radial velocity curves and obtained a set of spectroscopic elements.

Our previous analysis efforts (Milone, Stagg, & Schiller 1992b) involved only the mean light curve of Dugan & Wright without benefit of the spectroscopic solution. Subsequently, we have reanalyzed these data, those of Wachmann (1936), and a set of visual estimates of Kordylewski (Kordylewski et al. 1961), making use of the radial velocities to delimit properties of the system. The analysis of all available data sets marks an attempt to constrain the variation of the system's properties and to investigate the changing amplitude of the light variation with time.

This is not the first time that eclipse cessation has been seen. The visibility of eclipses depends upon the sizes of the eclipsing and eclipsed objects, the inclination of the orbital plane, and, in eccentric orbit cases, the eccentricity and orientation of the line of apsides. Occulting disks or shells are known to vary in size, and, usually on evolutionary timescales, and so may the stellar components themselves. Systems in which eclipse amplitude has been observed to vary include IU Aur (Harries, Hilditch, & Hill 1998; Schiller 1981), RW Per (Schaefer & Fried 1991), and, most recently, V907 Sco (Sandberg Lacy, Helt, & Vaz 1999), in which changing eclipse amplitudes have been attributed to the varying of the eclipsing binary orbital plane relative to the invariable plane involving the close binary and a more distant third star.

Among these other systems, the only one with possible (although disputed) cluster membership that has periodic eclipse seasons is V907 Sco (Sandberg Lacy et al. 1999). We will discuss the properties of the third component in the SS Lac system in § 4.

2. DATA

2.1. *Photometric Data*

Photometric observations were obtained with the automated, gated pulse-counting photoelectric photometry system (*RADS*) on the 41 cm telescope of the Rothney Astrophysical Observatory (see Milone et al. 1982; Milone & Robb 1983). Observations were made in U, B, V Johnson and R and I Cousins passbands relative to comparison star BD $+45°3771$ = SAO 51588 = HD 209482 in the 1982–1983 seasons and relative to comparison star BD $+45°3777$ = SAO 51617 = HD 209692 in the 1989–1991 seasons.

As with other RADS data, mean extinction coefficients have been found to be sufficiently accurate over the small range of secondary mirror chop (for SS Lac and the comparison star used in the 1990s, only $\sim 7'$), because of the typically small differential air mass (in this case, $\lesssim 0.0015^P$). Mean transformation coefficients were also applied, but zero points were not determined. The phasing was done with the elements of Dugan & Wright (1935): $E_0 =$ 2,415,900.76 and $P = 14.41629$ days, but for photometric purposes, phasing in the present era differs not at all from phasing with the recent ephemeris, that of Tomasella & Munari (1998), cited above. The mean values of the differential light curves for the interval JD 2,447,666–2,448,559 (1989–1991 seasons) are given in Table 1. Normalized light curves for the 1982–1983 and 1989–1991 seasons are shown in Figure 1, where they can be compared to the photographic light curve obtained by remeasurement of Harvard College Observatory (HCO) plates by S. J. S.

The mean values together with the absolute photometry of Hoag et al. (1961) for HD 209692 ($V = 8.53$, $B-V = 0.34$, $U-B = 0.16$) were added to our differential data to yield mean values of the SS Lac system in the 1990s of $V = 10.049 \pm 0.005$, $B-V = 0.169 \pm 0.006$, and $U-B = 0.129 \pm 0.006$, where a mean standard error (m.s.e.) of ± 0.005 has been assumed for the comparison star photometry. Standardization done by S. J. S. in the course of photometry carried out at the MacDonald Observatory (Schiller & Milone 1987) gave the following values

TABLE 1

SS LACERTAE RAO DIFFERENTIAL PHOTOELECTRIC MEANS

Magnitude/CI	1989	1990	1991	1989–1991
V	1.537 ± 0.005	1.505 ± 0.003	1.524 ± 0.002	1.519 ± 0.002
N_V	14	49	77	140
$B-V$	−0.171 ± 0.008	−0.162 ± 0.009	−0.172 ± 0.006	−0.171 ± 0.004
N_{B-V}	14	48	75	137
$U-B$	−0.046 ± 0.010	−0.029 ± 0.007	−0.031 ± 0.032	−0.031 ± 0.004
N_{U-B}	13	45	73	131
$V-R$	−0.096 ± 0.004	−0.087 ± 0.003	−0.087 ± 0.002	−0.088 ± 0.001
N_{V-R}	15	49	77	141
$V-I$	−0.144 ± 0.007	−0.139 ± 0.004	−0.139 ± 0.002	−0.140 ± 0.002
N_{V-I}	15	47	76	138

for comparison star BD +45°3771: $V = 9.125 \pm 0.018$, $B-V = 0.103 \pm 0.006$, $U-B = 0.101 \pm 0.009$, $V-R = 0.070 \pm 0.003$, $R-I = 0.078 \pm 0.003$, and $V-I = 0.138 \pm 0.005$. S. J. S. has computed mean SS Lac photometry for the 1982–1983 seasons: $V = 10.103 \pm 0.014$, $B-V = 0.166 \pm 0.005$, $U-B = 0.157 \pm 0.007$, $V-R = 0.099 \pm 0.001$, $R-I = 0.107 \pm 0.005$, and $V-I = 0.202 \pm 0.004$. To these we can add the photoelectric determinations of Lacy (1992): $V = 10.096 \pm 0.006$, $B-V = 0.160 \pm 0.003$, $U-B = 0.173 \pm 0.006$, and $N = 7$, over the two seasons 1989–1990, centered at JD 2,447,822, ~1989.8.

The weighted means of the three sets of UBV determinations are $\langle V \rangle = 10.071 \pm 0.017$, $\langle B-V \rangle = 0.163 \pm 0.003$, and $\langle U-B \rangle = 0.143 \pm 0.010$. The dispersion in V among the determinations provides mild evidence for small brightness variation in the system over a decade, but systematic effects in the more recent RAO photometry are more likely reasons for the differences, especially since the epochs of the S. J. S. and Lacy determinations, which are in relative agreement, are about a decade apart. The weighted means for these two sets alone are $\langle V \rangle = 10.097 \pm 0.003$, $\langle B-V \rangle = 0.162 \pm 0.003$, and $\langle U-B \rangle = 0.166 \pm 0.009$. These values are close to those reported by Hoag et al. (1961), themselves, for SS Lac, their star 4: $V = 10.09$, $B-V = 0.14$, and $U-B = 0.16$ from photoelectric photometry. Thus, $\langle B \rangle = 10.259 \pm 0.004$ for the system. These means have been adopted for the calculation of the absolute parameters of the SS Lac system.

The lack of eclipses in historically recent times requires any light-curve analysis to be carried out on earlier light curves. Literature searches for previous observations were carried out by Zakirov & Azimov (1990), who suggested eclipse cessation by the early 1950s, and by Mossakovskaya (1993), who concluded that eclipses must have ceased between 1935 and 1940. The archival data sets include the following:

1. Harvard College Observatory patrol camera plates; individual measures have not been published (see Dugan & Wright 1935); 1700 plates contained usable images of SS Lac. Of these, 790 plates had plate scales of 163″ mm^{-1} or better, and, of these 790 plates, 591 I-series plates taken between 1890 and 1939 were remeasured by Schiller, Bridges, & Clifton (1996).
2. 318 visual estimates by Hoffmeister at Sonneberg covering 293 nights between 1915 May 15 and 1918 October 31; unfortunately, only times of minimum, and an interesting sinusoidal ephemeris, were published.
3. 197 Bergedorf Observatory plates taken between 1929 May and 1932 December measured by Wachmann with a Leitz Double Microscope (Wachmann 1935, 1936).
4. 523 visual estimates with mainly f/11 or f/12 20 cm objective telescopes at Cracow and Warsaw between 1927 May and 1937 October (Kordylewski et al. 1961).
5. 25 plates taken with f/4.5 120 mm cameras of the Engelhardt Observatory between 1926 and 1932 (Nekrasova 1938).
6. Plates taken at the Crimean station of the Sternberg Institute with a 40 cm astrograph and from the Moscow station at *Krasnoi Presne* with f/6.6 9.7 cm and f/5 16 cm cameras (Mossakovskaya 1993); they cover the intervals (*a*) 1898 December–1911 August (26 plates); (*b*) 1935 August–1942 November (30 plates); (*c*) 1950 October–1957 Septem-

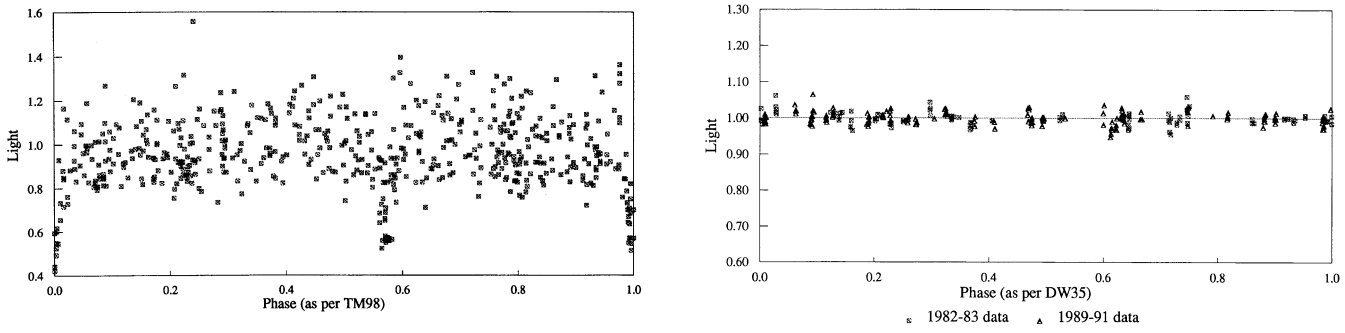

FIG. 1.—Photometry of SS Lacertae. *Left*, The light curve from a portion of the Harvard College Observatory database of plates remeasured by S. J. S.; *right*, photoelectric observations in the V passband for the 1982–1983 and 1989–1991 observing seasons, demonstrating the absence of eclipses in the modern era.

ber (40 plates); and (*d*) Sporadically through the interval 1968 September–1987 October (185 plates).

7. Sonneberg Sternwarte patrol camera plates taken between 1890 and 1989 (described by Lehmann 1991). These results have not been available generally and have not been used in the present study.

8. Finally, there is the published report of Tashpulatov (1965), who listed from 983 estimates from plates taken at the Tashkent Astronomical Observatory covering the range 1937 August–1955 May. We discuss these data and more recent estimates from them at length below.

There are problems with the archival data. Dugan & Wright (1935) published neither tables of their mean and raw light curves nor a diary of the individual plates. The Wachmann (1936) data, which are the most homogeneous in both time interval and light-curve scatter, lacks data on the falling branch and deep minimum of the secondary eclipse. Hoffmeister (1921) does not list any light curve measurements, while those of Kordylewski, Pagaczewski, & Szafraniec (1961) suffer from large scatter. No other published data set, except that of Tashpulatov (1965), which we discuss below, shows eclipses.

The normal points data plotted by Dugan & Wright (1935) were scanned by E. F. M. with an HPC-4 scanner at high resolution, printed at higher magnification, and measured with a Data Scales Inc. Variable Rule. Errors due to distortion and mismeasurement are judged to be no more than the uncertainty in the placement of the original data points, estimated at $\lesssim 0.02$ mag, and $\lesssim 0.002$ in phase. Only the second of two plottings of the primary minimum in the figure given by Dugan & Wright (1935) is symmetric and so these points were used for the final analysis. These measured and rescaled data, and others described here, are available on request in spreadsheet format. The measured values were then normalized to the mean of the data outside the minima, $\langle m_{pg}^{max} \rangle = 10.289 \pm 0.002$. On the advice of our referee, we have included the phased and normalized remeasured data as an aid to the reader.

To check the validity of the Dugan & Wright (1935) plot and to search for clues to the past behavior of the SS Lac system, Schiller et al. (1996) imaged all relevant plates with well-resolved images in the plate stacks at the Harvard College Observatory with a CCD video camera and frame grabber coupled to a 0.7×3.0 zoom microscope to produce for each plate image an eight-bit digitized record over a field of 512×512 pixels. The magnification permitted the comparison stars to be imaged on the higher resolution plates and subsequently measured. The plates with lower plate scales ($\sim 400''$–$700''$ mm^{-1}) were imaged but not measured because blending due to overcrowding on those plates made magnitude determination uncertain. Up to 16 stars were measured on each frame, but, depending on the degree to which seeing merged the images, between 8 and 12 were used for the differential photographic photometry. The comparison stars are listed in Table 2.

The HCO data sets, including that of Schiller et al. (1996), were normalized to the mean maximum value. For light-curve purposes, the latter data set was used to check mean light levels and to verify the placements of the minima. The Dugan & Wright mean data (hereafter DW35), plotted in units of days, were phased with the most recent elements (Tomasella & Munari 1998): $P_0 = 14.41638$ and $E_0 = 2450716.32$.

TABLE 2

COMPARISON STARS USED FOR THE HARVARD PLATE MEASURES[a]

X	*Y*	*V*	ID
−23.10.....	−15.88	8.53	BD +45°3771
+2.70	−8.57	10.26	
+0.70	−10.87	10.57	
−1.95	−6.30	10.61	
−10.36.....	+5.59	10.68	
−1.65	−2.73	10.68	
−6.62	−6.82	10.75	
−6.29	−11.17	10.95	
−16.41.....	−12.14	11.01	
−0.45	−10.54	11.08	
−13.96.....	−10.17	11.11	
+8.46	−3.82	11.37	
−5.87	+4.44	11.39	
−4.69	−2.48	11.73	
−9.34	−12.31	11.84	
−4.15	−0.63	12.01	

[a] Relative frame position and magnitude data from Hoag et al. 1961.

The remeasured HCO data demonstrate the presence of eclipses of large (~ 0.6 mag), but also possibly varying, amplitude. A plot is shown in Figure 1*a*. S. J. S. found that 55 of the measured plates occur within 0.015^P of mideclipse (for the analysis described in § 4, this condition was slightly relaxed to allow for the possibility of phase variation in the times of minima; we record 61 low-light entries). Of the 55, 37 are in the primary minimum, with 29 taken between 1890 and 1903, six between 1906 and 1907, and the remaining two in 1933. Of the 18 secondary minimum plates, 11 occurred before 1907 and six after 1923. The phases of minimum and maximum appear as in Dugan & Wright (1935); the primary minimum depth appears deeper here than in the Dugan & Wright (1935) normal points light curve, although the scatter is large. When all the data are considered, it is clear that the shape and depth of the mean plot of Dugan & Wright (1935) represent a composite of a family of light curves. The details of the cycle-by-cycle variation of the light curve revealed in the plate remeasures are in themselves interesting, and we will discuss them in § 4.

The HCO collection contains 90 plates of SS Lac at minimum, according to Dugan & Wright (1935). Since the remeasured set contains, in our current tally, only 61 low-light values, an important proportion of these data, albeit mostly from plates with less favorable plate scales, are still unavailable.

In contrast to the paucity of observational details given by Dugan & Wright, Wachmann (1936) conveniently provided mean and individual Bergedorf plate data, as well as a plot of the mean data. This is an invaluable set of high-quality data from a limited range of dates, permitting comparisons between early and late epoch properties of the system. Unfortunately, although the minima are certainly discernible, they are not so well covered as in the Dugan & Wright (1935) paper, especially the secondary minimum in which there are no points on the falling branch and only three on the rising branch. The individual observations of the Wachmann mean data set (hereafter W36), which included HJD values, were rephased with the Tomasella & Munari (1998) elements.

At one stage, the data of Wachmann (1936) were combined and modeled together with the Dugan & Wright data in order to obtain fuller light curve coverage since the range of dates spanned by the two sets overlap (Milone & Schiller 1998). However, subsequent work revealed that modeling is better carried out on the individual sets: first, because of a slight phasing offset between the two sets of data resulting in an apparent widening of the primary minimum in the combined set, and second, because of the effectively different mean light-curve properties encompassed by the two sets of data. Wachmann (1936) himself commented on the apparent phase shift (~ 0.1 day) between his minimum and that in the Dugan & Wright (1935) epoch and was puzzled by it, given the large range of dates of the plates that were used by Dugan & Wright (1935) to obtain their mean light curve. As a consequence, in the present analyses the data sets have been treated separately. The tabulated individual observations as well as the mean data values of Wachmann were normalized (to 9.998, in maximum light).

The data published in Kordylewski et al. (1961) overlap those of Wachmann. The Szafraniec compilation is the only currently available set of nonphotographic data that include eclipse observations. Of these, Szafraniec's own observations are few; the 114 visual estimations of Pagaczewski have a m.s.e. of a single observation, $\sigma_1 = 0.088$ at maximum light; and Kordylewski's 402 estimates have $\sigma_1 = 0.065$ (again deduced from the residuals about the mean at maximum light phases). Both the Pagaczewski and Kordylewski sets were examined for low-light values, but Kordylewski's larger and less noisy data set (hereafter K) was used for visual light-curve modeling trials. The data were normalized to maximum light and means were taken of every 10 data points at maximum light; the m.s.e. of the means were used to compute light-curve weights for the modeling.

The list published by Tashpulatov (1965) contains faint magnitude estimates for several minima. The last deep minimum (~ 0.5 mag below maximum) is given for JD 2,423,200, in 1949. He included a mean light curve that shows relatively low scatter and that disagrees with those of Dugan & Wright (1935) and Wachmann (1936) only in the amplitude of the variation, which he gave as 0.52 (Tashpulatov 1965), versus 0.41 mag in the other two sources. In contrast, the data sets examined by Mossakovskaya (1993) show very few faint data points after the 1930s. Indeed, Mossakovskaya (1993) considered the entire set of data presented by Tashpulatov (1965) to be unreliable and excluded it from her own analysis. According to M. Zakirov (1998, private communication), reliable estimates from the Tashkent plates are difficult to make because of the low plate scale of the camera and the fact that the cluster lies near the edge of many of the plates; nevertheless, a series of plate estimates recently made by I. M. Ischenko has been kindly provided by M. Zakirov (1998, private communication). They span the interval 1937–1950 and confirm that no minima can be attributed with any degree of certainty to the system after 1937. We will discuss these estimates further in § 4.

As noted, each of the archival light curves presents impediments to analysis: the DW35 data are complete but are averaged over too great a range of dates to establish a unique and reliable inclination, for example. The scatter in remeasured HCO data over limited ranges of dates is too great to yield results significant enough to throw much additional light on the modeled parameters (although the level of scatter is interesting in itself and will be discussed in § 4). The W36 data set suffers from an incomplete secondary minimum, and the Kordylewski et al. (1961) sets have too high scatter for precise determinations of most parameters. Nevertheless, the data sets DW35, W36, and K are the only light-curve data usable for the analyses described in the next section, and so we attempt to analyze them as fully as possible. Independently of the light-curve analysis, minima in the full data sets of the remeasured Harvard archival data, and in other published data, have been examined, resulting in a characterization of the variation of the depth of the minima.

2.2. *Spectroscopy*

Radial velocity observations of SS Lac were made by S. J. S. in 1983–1984 at DAO with the 1.8 m telescope with a single-stage image-intensifier and both photographic plates and Reticon detector. Twelve observations were obtained with 15 Å mm^{-1} nominal reciprocal linear dispersion. The data were reduced and analyzed with the REDUCE and VCROSS software of Hill, Fisher, & Poeckert (1982) and Hill (1982), respectively. The cross-correlated radial velocities are given with respect to comparison star HD 27962 (A3 V or A2 IV); δ Tau, the radial velocity of which Wilson (1963, p. 52) gives as $+34.7$ km s^{-1}. The results of this first spectroscopic work were reported by Schiller & Milone (1996) to be negative, in the sense that the radial velocity did not appear to vary significantly from the gamma velocity, which was determined to be -24.9 ± 4.8 km s^{-1} (excluding the datum from plate 92593, discrepant from the others but taken at nearly the same phase as another point close to the average). These data are summarized in Table 3. The phasing is that of Dugan & Wright (1935).

Subsequently, Etzel et al. (1996), Etzel & Vogelnau (1996), and Stefanik et al. (1996) reported a clear doubling of the lines, and Tomasella & Munari (1998) produced a radial velocity curve for each component. The mean value of Schiller & Milone (1996) is not significantly different from either the gamma velocity determined here (-19.9 ± 0.8) or by Tomasella & Munari (1998) (-21.2 ± 0.3) or the value for a third component seen at quadratures (-22.3 ± 3.0 km s^{-1}) found by Tomasella & Munari (1998).

P. B. Etzel (1998, private communication) reports that the doubling of lines is seen in metal lines in the blue region of

TABLE 3

SS Lacertae Archival Radial Velocity Data

Plate	HJD	Phase[a]	RV[b]
91997.....	2,445,546.9615	0.438	−69.04
91998.....	2,445,546.9878	0.439	−60.98
92004.....	2,445,547.7552	0.493	−52.52
92012.....	2,445,548.7587	0.562	−63.85
92014.....	2,445,548.7670	0.563	−54.26
92593.....	2,445,710.6806	0.794	−33.86
92954.....	2,445,710.6895	0.795	−58.81
92957.....	2,445,711.6562	0.862	−59.54
93370.....	2,445,918.8792	0.236	−60.26
93371.....	2,445,918.8882	0.237	−53.34
93372.....	2,445,918.8988	0.237	−51.15
93380.....	2,445,919.0257	0.246	−62.64

[a] Phased as per Dugan & Wright 1935.

[b] Relative to HD 27962.

the spectrum. Tomasella & Munari (1998) measured the radial velocity variation only in the Balmer lines in their echelle spectra, which covered the range from Hα to Hγ, because the weakness of the other lines precluded reliable measurements from them.

A reexamination of tracings of the spectra obtained by S. J. S. does not reveal any clear-cut evidence of this doubling even in the Balmer lines, which were systematically masked off for the cross-correlation procedure (a standard practice because inclusion of the broad and often blended Balmer lines tends to broaden rather than sharpen CCF peaks), although a suggestion is present in some cases. The doubling is certainly visible in the cores of the Balmer lines of spectra taken subsequently at DAO with the same camera on DAO'S 1.8 m telescope with unintensified CCD detectors. These new spectra are not reduced at present writing, but the separations of the cores at quadratures do confirm the results of Tomasella & Munari (1998) and others. Thus, our earlier failure to detect doubling can be attributed to insufficient S/N possibly coupled with resolution problems in our data.

The spectra also provide temperature estimates that are needed for light-curve modeling. Tracings of our DAO spectra (which reveal weak lines of $\lambda\lambda$4227 and 4233, as well as other metal lines and a depth of the Ca K line $\sim\frac{2}{3}$ that of Ca H + Hϵ) suggest a spectral type between A3 and A4, while Tomasella & Munari (1998), on the basis of the strong wings of the Balmer lines, suggest A2. The temperature scale tabulated by Popper (1980) was used to provide temperature estimates. With initial temperature values for both spectral type estimates (i.e., A3.5 and A2) and T_2 adjusted with the temperature difference found from preliminary modeling trials of the DW35 data, a best value of $T_1 = 8732$ K, just slightly cooler than the temperature scale predicts for an A2 classification, was obtained. However, this result was derived for models which were not fully consist with the information supplied by Tomasella & Munari (1998). Consequently, for most of the final modeling, which is described below, $T_1 = 8750$ was adopted, appropriate for a star of A2 spectral class (Popper 1980). We next describe the analysis of the Tomasella & Munari (1998) data with our light and velocity modeling program, WD93K93.

3. ANALYSES

3.1. *Radial Velocity Analyses*

To begin the analyses, the radial velocity data of Tomasella & Munari (1998, hereafter TM98) were reanalyzed with WD93K93c, a University of Calgary version of the Wilson-Devinney (WD) program. All light and radial velocity curves were modeled in mode 2, appropriate for detached systems. Albedo and gravity-darkening coefficients were set at 1.0 for these early-type stars with presumed radiative envelopes, and the atmospheres option with Kurucz (1993) atmospheres for the component stars was invoked for all trials. Solar [Fe/H] values were assumed, and given the relatively low quality of the analyzed light-curve data, no other compositions were explored. All models indicate that the stars are well separated with negligible radiative interaction. Consequently, simple (single-pass) reflection was used for all modeling.

The procedure was as follows: The radial velocity curve of each component was analyzed separately to convergence, yielding consistent values of the parameters V_γ (the barycentric velocity) and *Pshift* (phase shift). The latter is the phase increment to a synthetic light curve required to match the phasing of the observations.

The RV curves were then modeled together. The initial parameters (in the Wilson 1992 conventions) were those determined by TM98, viz., the projected semimajor axis in solar radii, $a \sin i = 42.5$; eccentricity, $e = 0.122$; argument of periastron, $\omega = 332°$; the barycentric velocity, $V_\gamma = -21.2$ km s^{-1}; and mass ratio, $q = M_2/M_1 = 1.041$. In addition, *Pshift* or $\Delta\phi$ was assumed to be zero initially, and the inclination, i, was fixed at 78° as per TM98. The assumed photometric parameters were the preliminary set determined by Milone & Schiller (1998) for the Dugan-Wright data. The data were weighted by the inverse of the error cited in TM98, but with zero weight given data just outside the conjunctions, where blending may have been a problem. Data at the conjunctions were given full weight.

A critical step for analysis is the identification of the star eclipsed at primary minimum (phase 0.0), star 1 in Wilson-Devinney usage, with the TM98 star "b." Star 2 is thus TM98's star "a." The radial velocity and spectral plots of TM98 leave no doubt that this is the case. In all modeling, *Pshift* (applied to the computed light curve) was adjusted. Other adjusted parameters were a, e, ω, q, and V_γ. Adopted and unadjusted values for some of the other parameters are given along with the RV-fitting results in Table 4; the fitting results can be seen in Figure 2.

While not identical (the parameters were started at the TM98 values and consistently moved to new values in all trials), the parameters are seen to be not significantly different from those of Tomasella & Munari (1998), but the formal uncertainty in a single RV datum of average weight, equivalent to the uncertainty in the RV curve fitting, is larger (± 4 vs. ± 0.8 km s^{-1}). The phasing with the period of Tomasella & Munari (1998) is essentially consistent with minima as computed with the Dugan & Wright (1935) ephemeris; low-light data in the minima seem to be well phased in the remeasured HCO data, for instance. Consequently, no new determination of phase elements was attempted. The phasing is such that at phase 0.00 the star undergoing eclipse (star 1 in the Wilson-Devinney convention) is the less massive star (star b of Tomasella & Munari 1998). Thus, $q > 1$.

Following each of the iterations, the RV modeling results were tested with the simplex option in our code, which automatically iterates until the stopping criteria are met: when either the fitting error or each parameter error decreases to a specified target level, or when the maximum

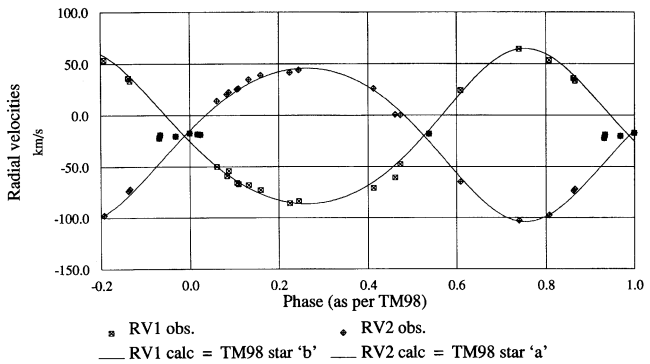

FIG. 2.—Radial velocity curve fitting. The data of Tomasella & Munari (1998) are shown, with the Wilson-Devinney model fitting.

TABLE 4

SS LACERTAE RADIAL VELOCITY SOLUTIONS[a]

Parameter (Units) (1)	WD Analysis[b] (2)	WD Analysis (i Optimized)[b] (3)	TM98[c] (4)
a ($R_\odot$)	43.06 ± 0.84	43.32 ± 0.84	42.5 ± 0.5
e	0.122 ± 0.017	0.122 ± 0.017	0.122 ± 0.019
ω (deg)	353.8 ± 6.4	353.9 ± 9.4	332 ± 9
$\Delta\phi$ (P)	0.0072 ± 0.0029	0.0072 ± 0.0029	...
V_γ (km s^{-1})	−19.85 ± 0.82	−19.85 ± 0.82	−21.3 ± 0.3
q	1.00830 ± 0.03538	1.00868 ± 0.03537	1.038 ± 0.022
i (deg)	78.0[d]	76.5	78.0
T_1[d] (K)	8732	8750	...
T_2[d] (K)	9036	8542	...
Ω_1[d]	18.7973	19.3537	...
Ω_2[d]	13.4410	13.1583	...
L_1^V[d] (4π)	8.7626	3.5939	...
$x_{1,2}^V$[d]	0.473, 0.484	0.473, 0.484	...
Σwr^2	22.391237	22.344299	...
σ_1	±0.044580	±0.044534	...

[a] Uncertainties in this table are standard deviations.
[b] Starting parameters as per Tomasella & Munari 1998 or Table 6.
[c] Tomasella & Munari 1998 $a \sin i$ is given.
[d] Assumed and unadjusted.

number of simplex iterations is reached, whichever is achieved first (see Kallrath 1993; Kallrath & Milone 1999, p. 160). For the best-fit model, the parameter differences fell below the target levels by at least an order of magnitude in each parameter. Modeled RV results are shown in columns (2) and (3) of Table 4. These results were used in the modeling of the light curves. Column (3) contains the final models, multiply iterated with the final model for DW35. The RV iterations are discussed further in § 3.2.1.

As we note in § 4, when the light-curve modeling results were achieved, the converged parameters were put back into the RV input file and again iterated to convergence (the inclination was fixed at 78° for most RV trials). The assumed luminosity of star 1 is for the V passband, which best corresponds to the wavelength region of the TM98 spectra. The luminosities in the V passband were computed on the bases of $T_{1,2}$, the reddened color indices, and B passband luminosities from the DW35 modeling.

Another series of modeling trials was done in which the inclination was fixed to a different value and the light curves modeled to convergence in each case. WD95, a self-iterating, damped–least squares version of our Wilson-Devinney light curve modeling code was used to speed up these trials. A local minimum was found for $i = 76.^\circ5$. Even lower fitting errors were found for higher inclinations (for example, $i = 84°$), but these were rejected as unphysical since no eclipses are currently seen (eclipses cease at $i \lesssim 82°$). The results and uncertainties are indicated in Table 4.

One would have liked to combine radial velocity and light curves for the final analysis. The problem, of course, is that the radial velocity curve and photometric parameters apply to separate epochs when at least one of the properties of the system was clearly different. The sets were therefore treated separately and iterated in various ways to achieve sets of mutually consistent results. We now discuss the light curve modeling.

3.2. *Light-Curve Analyses*

The most critical light curve data are the DW35 set. Table 5 contains the normalized means of this data set in the approximate format of the input files, arranged in five triads of phase, light, and weight. The phases were computed from the TM98 ephemeris, the light is normalized to the mean of the maximum, and the weights were assigned to give higher weight to data in the minima, as noted below. The tools used for the analyses were the University of Calgary versions of the Wilson-Devinney code (Wilson 1992; Milone, Stagg, & Kurucz 1992a; Stagg & Milone 1993; Kallrath et al. 1998) and auxiliary software used to summarize and visualize output.

Starting values for such parameters as e and ω, in various trials included both the TM98 parameters and those found from our own RV trials. The differential corrections subprogram of the Wilson-Devinney consistently moved the values from these initial values. Attempts to adjust i from the assumed value of 90° proved unsuccessful in the initial modeling, with unphysically large positive adjustments indicated. The situation was circumvented with the inclination fixed at a different value for each of a subseries of runs, as per the radial velocity curve trials discussed above. When convergence was achieved in each fixed-inclination subset of each subseries, a new value of the inclination was selected, and the process was repeated. The range of i explored was 84°–90°. This was important because we show in § 4 that the amplitudes of the minima in the 1920s and 1930s varied over timescales of years or less.

Solutions were tested with our simplex option (since the convergence method is different for the Wilson-Devinney and simplex codes), and the converged solutions were found to be within the errors of the WD determinations. The effects of different inclinations were tested in three other series of extensive runs with a self-iterating, damped–least squares version of WD93K93, WD95 (Kallrath et al. 1998; Kallrath & Milone 1999, p. 219).

The light-curve fitting parameters for all three light-curve data sets were run until self-consistent with limb-darkening values derived from Kurucz (1993) atmospheres incorporated in a table provided by W. van Hamme (1996, private communication). Values of log g were continually updated also during the iteration process. The final models are

TABLE 5

INPUT DATA USED FOR THE DW35 SET LIGHT-CURVE MODELING[a,b]

ϕ[c]	l	w	ϕ[c]	l	w	ϕ[c]	l	w	ϕ[c]	l	w	ϕ[c]	l	w
0.0137.....	0.9716	1	0.0207.....	0.9897	1	0.0311.....	1.0076	1	0.0401.....	1.0081	1	0.0574.....	0.9979	1
0.0727.....	0.9851	1	0.0831.....	0.9988	1	0.0914.....	1.0174	1	0.1046.....	0.9970	1	0.1164.....	1.0099	1
0.1358.....	0.9671	1	0.1504.....	1.0081	1	0.1587.....	1.0034	1	0.1649.....	0.9851	1	0.1733.....	1.0062	1
0.1913.....	0.9979	1	0.2010.....	1.0127	1	0.2093.....	1.0127	1	0.2183.....	0.9879	1	0.2260.....	1.0025	1
0.2336.....	0.9924	1	0.2392.....	1.0007	1	0.2475.....	0.9860	1	0.2565.....	1.0025	1	0.2711.....	1.0007	1
0.2856.....	0.9869	1	0.2912.....	0.9779	1	0.2981.....	0.9998	1	0.3148.....	1.0155	1	0.3252.....	1.0118	1
0.3363.....	1.0034	1	0.3522.....	1.0430	1	0.3668.....	1.0081	1	0.3786.....	0.9521	1	0.3855.....	1.0230	1
0.4022.....	1.0306	1	0.4105.....	1.0430	1	0.4174.....	0.9952	1	0.4375.....	0.9897	1	0.4493.....	0.9988	1
0.4542.....	1.0382	1	0.4583.....	1.0146	1	0.4688.....	1.0230	1	0.4757.....	0.9970	1	0.4916.....	1.0146	1
0.4965.....	0.9770	1	0.5069.....	0.9897	1	0.5236.....	0.9924	1	0.5437.....	0.9947	1	0.5516.....	1.0025	9
0.5579.....	0.8247	5	0.5607.....	0.7721	9	0.5631.....	0.7313	9	0.5624.....	0.7055	9	0.5638.....	0.6797	9
0.5707.....	0.6666	1	0.5686.....	0.6828	1	0.5700.....	0.6917	1	0.5745.....	0.7019	1	0.5673.....	0.7104	1
0.5770.....	0.7156	9	0.5822.....	0.9089	5	0.5877.....	0.9730	5	0.6016.....	1.0123	1	0.6163.....	1.0425	1
0.6255.....	0.9970	1	0.6387.....	0.9915	1	0.6463.....	1.0165	1	0.6630.....	0.9952	1	0.6762.....	1.0090	1
0.6886.....	0.9851	1	0.7088.....	0.9806	1	0.7205.....	0.9788	1	0.7296.....	0.9851	1	0.7532.....	0.9942	1
0.7642.....	0.9797	1	0.7747.....	0.9897	1	0.7823.....	0.9860	1	0.7913.....	0.9988	1	0.8003.....	1.0034	1
0.8142.....	0.9833	1	0.8267.....	1.0109	1	0.8412.....	0.9952	1	0.8641.....	0.9897	1	0.8780.....	0.9779	1
0.8898.....	1.0062	1	0.9016.....	0.9860	1	0.9155.....	0.9970	1	0.9259.....	1.0044	1	0.9342.....	1.0044	1
0.9470.....	1.0174	1	0.9640.....	0.9783	1	0.9769.....	0.9728	5	0.9862.....	0.9084	5	0.9890.....	0.7869	9
0.9904.....	0.7337	9	0.9914.....	0.7127	9	0.9921.....	0.7213	9	0.9942.....	0.7045	9	0.9963.....	0.6863	9
0.9989.....	0.6759	9	0.0032.....	0.6768	9	0.0008.....	0.6910	9	0.0046.....	0.7127	9	0.0088.....	0.7256	9
0.0157.....	0.9689	5	0.0237.....	0.9915	1	0.0341.....	1.0091	1	...	...	...	...	...	...

[a] Data remeasured from figure in Dugan & Wright 1935.
[b] See § 3.1 for details.
[c] Phasing as per Tomasella & Munari 1998.

shown in Table 6 for the DW35 data set, Table 7 for the W36 set, and Table 8 for the K set. The data and best-fitting models are shown in Figure 3. The relative luminosities given for the DW35 and W36 models are for the B passband; that for the K model is for the V passband. Since the DW35 fitting is the most critical, the primary and secondary minima are shown in detail.

3.2.1. *Analyses of the Dugan-Wright Data Set*

For the DW35 analysis, assumed values included a, V_γ, and q from the RV modeling. The adjusted values were e; ω; $\Delta\phi$; temperatures of star 1 (in earlier trials) and 2, $T_{1,2}$; modified Roche potentials, $\Omega_{1,2}$; luminosity of star 1 (in units of 4π), L_1; and third light, l_3.

TABLE 6

SS LACERTAE LIGHT-CURVE MODELING SOLUTIONS FOR DW35 SET[a,b]

Parameter (Units) (1)	Model 1[c] (2)	Model 2[d] (3)	Final Model[e] (4)
a[f] ($R_\odot$).....	42.83	43.45	43.32
e.....	0.1269 ± 0.0017	0.1226 ± 0.0049	0.1106 ± 0.0014
ω (deg)	330.59 ± 4.97	334.46 ± 4.85	354.54 ± 7.34
$\Delta\phi$ (P)	0.0359 ± 0.0004	0.0356 ± 0.0003	0.0346 ± 0.0004
V_γ[f] (km s^{-1}).....	−19.70	−21.20	−19.85
q[f].....	0.9851	1.0410	1.00868
i[f] (deg)	89.9 ± 7.7	90.0 ± 4.6	90.0
T_1[f] (K)	8732	8732	8750
T_2 (K)	9013 ± 306	9036 ± 308	8542 ± 304
Ω_1.....	12.708 ± 0.169	13.083 ± 0.188	19.354 ± 0.097
Ω_2.....	18.900 ± 0.526	20.647 ± 0.666	13.158 ± 0.166
L_1 (4π).....	8.680 ± 0.350	8.690 ± 0.356	3.957 ± 0.050
l_3 (unity)	0.000 ± 0.026	0.000 ± 0.030	0.000 ± 0.017
$x_{1,2}^{\rm bol}$[f]	0.570, 0.539	0.569, 0.588	0.574, 0.564
$x_{1,2}^{B}$[f]	0.572, 0.539	0.574, 0.539	0.561, 0.585
Σwr^2	0.137132376	0.135772198	0.126630291
σ_1	0.022897	0.022784	0.022003

[a] The uncertainties in this table are probable errors, as per WD output.
[b] Data from Dugan & Wright 1935.
[c] $T_1 < T_2; L_1 > L_2; q < 1$
[d] $T_1 < T_2; L_1 > L_2; q > 1$
[e] $T_1 > T_2; L_1 < L_2; q > 1; a = 43.316\ R_\odot$ from RV-optimized $i = 76.^\circ5$ model.
[f] Assumed and unadjusted; or readjusted only for T and log g changes; $e_{T_1} = \pm 300$ assumed.

TABLE 7

SS LACERTAE LIGHT-CURVE MODELING SOLUTIONS FOR W36 SET[a,b]

Parameter (Units)	Model 1[c]	Model 2[d]	Final Model[e]
a^f ($R_\odot$)	42.83	43.45	43.06
e	0.127 ± 0.023	0.128 ± 0.028	0.121 ± 0.005
ω (deg)	339 ± 23	338 ± 28	358 ± 30
$\Delta\phi$ (P).....	0.0268 ± 0.0029	0.0271 ± 0.0029	0.0264 ± 0.0025
$V_\gamma{}^f$ (km s^{-1}).....	−19.70	−19.80	−19.85
q^f	0.9851	1.00830	1.00868
i (deg)	88.3 ± 1.2	88.2 ± 1.2[f]	88.6 ± 1.3[f]
T_1 (K)	8732 ± 530	8732[f]	8750[f]
T_2 (K)	9013 ± 598	9190 ± 414	8542[f]
Ω_1	12.89 ± 0.70	13.26 ± 1.40	19.93 ± 2.45
Ω_2	19.83 ± 2.87	20.09 ± 2.43	14.33 ± 1.21
L_1 (4π)	8.671 ± 1.748	8.475 ± 1.895	3.724 ± 0.455
l_3 (unity)	0.019 ± 0.098	0.001 ± 0.093	0.130 ± 0.119
$x_{1,2}^{bol\,f}$	0.570, 0.589	0.569, 0.588	0.574, 0.564
$x_{1,2}^{B\,f}$	0.572, 0.539	0.574, 0.539	0.561, 0.584
Σwr^2	0.191972	0.005140	0.008183
σ_1	0.0366	0.0359	0.0378

[a] The uncertainties in this table are probable errors.
[b] Data from Wachmann 1936.
[c] $T_1 < T_2$, ; $L_1 > L_2$, $q < 1$; $e_{T_{1,2}}$ when i, other T unadjusted; e_i when T unadjusted.
[d] $T_1 < T_2, L_1 > L_2, q > 1$; T_2 adjusted.
[e] $T_1 > T_2, L_1 < L_2, q > 1$; $T_{1,2}$ fixed at DW35 model 3.
[f] Fixed or readjusted only for T and log g changes.

The parameters, e, ω, $\delta\phi$, $T_{1,2}$, $\Omega_{1,2}$, L_1, and l_3, were adjusted until the changes were essentially ignorable in all uncorrelated subsets, i.e., until the adjustments had too few significant figures to affect the input file parameters. Except for the simplex and WD95 runs, which iterate until the precision equals that of the input data, the resulting solutions were therefore converged to a higher degree than most modeling runs.

The data at deep eclipses were weighted at 9.0, those on the shoulders, 5.0, and those at maximum (where the overwhelming bulk of the data lay), at 1.0. Such a scheme was necessary so that the scatter in the data at maximum light did not overwhelm the relatively few points in the actual minima.

Several series of trials were undertaken, both before and after the TM98 data set became available. Three main sets of these trials can be characterized as follows:

Model 1.—$T_1 > T_2, L_1 > L_2, q < 1$.
Model 2.—$T_1 < T_2, L_1 > L_2, q > 1$.
Model 3 (Final).—$T_1 > T_2, L_1 < L_2, q > 1$.

TABLE 8

SS LACERTAE LIGHT-CURVE MODELING SOLUTIONS FOR K DATA SET[a,b]

Parameter (Units)	Model 1[c]	Model 2[d]	Final Model[e]
a^f ($R_\odot$)	42.83	43.45	43.316
e	0.148 ± 0.025	0.145 ± 0.017	0.126 ± 0.007
ω (deg)	331 ± 17	333 ± 14	354 ± 29
$\Delta\phi$ (P).....	0.0276 ± 0.0016	0.0247 ± 0.0016	0.0255 ± 0.0021
$V_\gamma{}^f$ (km s^{-1}).....	−19.70	−21.20	−19.85
q^f	0.9851	1.0410	1.00868
i^f (deg)	90	90.0	88
T_1 (K)	8796 ± 236	8732[f]	8750[f]
T_2 (K)	8654 ± 215	9036 ± 350	8198 ± 185
Ω_1	12.982 ± 0.664	15.478 ± 0.533	21.140 ± 0.869
Ω_2	22.865 ± 3.232	29.947 ± 5.702	13.591 ± 0.716
L_1 (4π)	8.680 ± 1.934	8.869 ± 2.656	2.935 ± 0.155
l_3 (unity)	0.131 ± 0.152	0.096 ± 0.208	0.272 ± 0.050
$x_{1,2}^{bol\,f}$	0.570, 0.564	0.571, 0.590	0.574, 0.564
$x_{1,2}^{V\,f}$	0.481, 0.484	0.478, 0.454	0.473, 0.484
Σwr^2	0.134630	0.003831	0.003290
σ_1	0.05384	0.05449	0.05149

[a] The uncertainties in this table are probable errors.
[b] Data from Kordylewski et al. 1961.
[c] $T_1 > T_2$; $L_1 > L_2$; $q < 1$; $e_{T_{1,2}}$ is for ΔT when the other T is adjusted.
[d] $T_1 < T_2$; $L_1 > L_2$; $q > 1$; T_2 fixed.
[e] $T_1 > T_2$; $L_1 < L_2$; $q > 1$; T_2 adjusted.
[f] Assumed and unadjusted or readjusted only for T and log g changes.

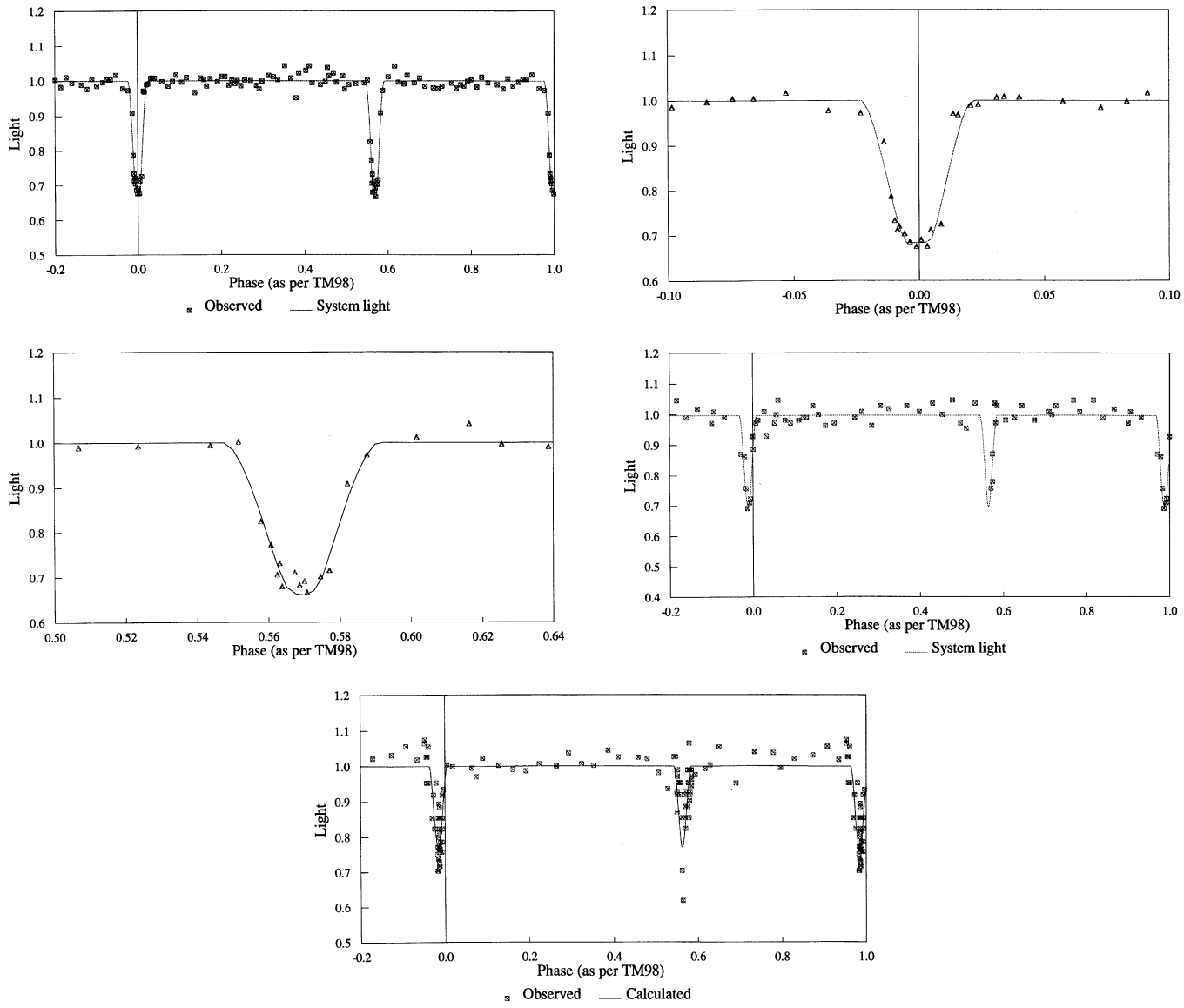

FIG. 3.—Fittings to the normalized mean photographic light curves of Dugan & Wright (*top left*, *top right*, and *middle left*), Wachmann (*middle right*), and the visual estimates of Kordylewski et al. (1961; *bottom*. See text for details.

Model 1, the pre-TM98 model, had a larger modified Roche potential (and therefore smaller radius) for star 2 and with temperature $T_1 > T_2$. In the earliest modeling, T_1 was taken to be 10,000 K on the strength of the A star classification of Cannon (Dugan & Wright 1935) and the B9 V classification of Svolopoulos (1961). Except for an early set of trials (noted below) in which both temperatures were adjusted, the modeling proceeded with T_1 fixed, resulting in smaller uncertainties for T_2 and the other elements. The best solution for this model is seen in column (2) of Table 6. A number of subsequent trials were carried out by trying a succession of inclination values and plotting the Σwr^2 of the converged solutions. The best-fitting solution was found to be 89°.9.

Our own spectral classification, as noted above, suggested a spectral type somewhat later than A2. From the temperature scale adopted by Popper (1980), $T_1 \approx 8700$ K, which after some preliminary modeling of T_1, converged to 8732 K. This model, model 2, and the realization that star b of Tomasella & Munari (1998) was equivalent to star 1 in Wilson-Devinney modeling code usage, compelled us to use a mass ratio greater than 1, since the more massive component is star a in the Tomasella & Munari (1998) solution. Since the masses are nearly equal, however, this change does not critically affect most parameters, as comparison between this solution, column (3) of Table 6, and the adopted solution (col. [4]) shows. That model 2 is unlikely to be correct is demonstrated by the circumstance that iterations between the RV and light-curve input parameters would not result in improved fitting; rather, the reverse occurred. In these iterations, the best-fit adjusted parameters unique to the light-curve modeling were inserted into a second round of RV modeling; the best-fit adjusted parameters unique to the RV modeling (namely, a, V_γ, and q) were then put into the previously converged light-curve model, and a new round of trials begun to convergence. However, for this model, such convergence resulted in higher fit error. Consequently, the model shown in column (3) of Table 6 is the uniterated solution. This model has the additional flaw that it does not agree with the luminosity estimates of

Tomasella & Munari (1998), which indicate that star a (our star 2) is slightly more luminous than star 1. No rigorous attempt was made to optimize the inclination for this model, but some trials suggested that $i = 90°$ was the likely optimum value.

Model 3 adopts the Tomasella & Munari (1998) relative luminosity assessment and spectral type estimates, A2 V. Again from Popper (1980), we adopted a temperature $T_1 = 8750$ K. To minimize the difference in luminosity and size between the components (since Tomasella & Munari 1998 argue that the sizes are not greatly different), we assume star 1 to be the hotter component in this model. The fitting errors are not greatly different for this model but are better than for models 1 and 2. Model 3, moreover, could be iterated with the RV model to produce improved and consistent fittings with both RV and light curves. Three iterations resulted in the mutually consistent solutions. The inclinations for most of the trials of this model were fixed at 90°, but the sensitivity of the adopted solutions to both past and present inclination was also explored. After the third-iteration TM98 trials were completed, the inclination alone was changed successively over the range 64°–84° and with the new, fixed value of i, the model was rerun (with the same parameters adjusted as in other trials) until all adjustments were ignorable in all subsets (which usually occurred in a few iterations or less).

The variation of i in RV curve fitting mainly acts to alter a, with occasional adjustments to the other parameters. Although the inclination cannot be determined from RV data alone, the light-curve results from the third iteration were included in these trials; as noted in § 3.1, the results indicated a preference for higher inclinations, with the best RV fittings occurring at inclinations of 84° (the limit of the trials), where $\sigma_1 = \pm 0.044492$. However, this inclination would require present-day eclipses, which are not seen; thus, this result had to be rejected as nonphysical. We return to this in a later section. A secondary minimum in the plot of Σwr^2 is seen at $i = 76\overset{\circ}{.}5$, for $a = 43.316\ R_\odot$. When this value of a was inserted in the DW35 third iterated solution input file, no further improvement was seen. Finally, the same type of inclination trials was performed on the model 3 solution, except that they were carried out with WD95, since previous experience suggested that convergence for each new inclination value might be lengthy, especially at the lower inclinations. These trials showed a clear minimum at $90\overset{\circ}{.}0$, even when probed as close to 90° as $89\overset{\circ}{.}95$. With these trials concluded, no further runs were needed, since the solution now appeared to be consistent and optimum, as far as the data and model allowed. Model 3, with the new value of a from the TM98 i tests, was taken as the adopted model, the properties of which are shown in column (4) of Table 6 (see top left, top right, and middle left panels of Fig. 3).

3.2.2. *Analyses of the Wachmann Data Set*

The W36 data were weighted in similar fashion to the DW35 data. A directly analogous series of models was run:

Model 1.—$T_1 < T_2, L_1 > L_2, q < 1$.

Model 2.—$T_1 < T_2, L_1 > L_2, q > 1$.

Model 3.—$T_1 > T_2, L_1 < L_2, q > 1$, T_1, T_2 fixed at final DW35 model.

The models had the following differences:

1. Model 1: the inclination was optimized with $i = 88\overset{\circ}{.}328$.

2. Models 1 and 2: T_1 and T_2 were taken from the corresponding DW35 models, since the paucity of data in the secondary minimum in the W36 set likely precludes reliable determinations (a considerable effort was made to check this conclusion, as noted elsewhere).

3. Model 3: For this model the optimized inclination was found to be $i = 88\overset{\circ}{.}6$.

In all model runs, attempts were made to adjust i in at least some of the subset trials. Two sets of model 3 were run, both with fixed $T_1 = 8750$ as per DW35, but one with fixed $T_2 = 8542$ and a second in which T_2 was allowed to vary from this initial value. The latter set had a lower fitting error, $\sigma_1 = \pm 0.0364$ but higher parameter uncertainties (e.g., $T_2 = 9374 \pm 3220$), as expected. The model 3 fitting with fixed T_2 is shown in the middle right panel of Figure 3; the corresponding parameters are given in Table 7.

The similarity in parameters to the DW35 model, as well as the approximately equal depths of ~ 0.41 mag for the DW35 set, and the same depth for the primary minimum in the W36 set, lead us to conclude that we have no significant evidence for any change in the *mean* properties of the system between the early 1900s and the mid-1930s with the exception of the inclination and the shift of the minimum, noted earlier by, for example, Wachmann (1936). Such a view would be supported also by the observation of Hoffmeister (1921) that the range of light variation was ~ 0.4 mag and by the absence of any extended totality (i.e., $d \approx 0$).

3.2.3. *Analyses of the Kordylewski Data Set*

The modeling results for the Kordylewski subset of the data in Kordylewski et al. (1961) are presented as well. The observations of the K set at maximum light were averaged in groups of 10 consecutive phase-ordered data points, and weights were determined by the standard error of the mean of these averaged points.

The V-passband atmospheres correction was used for the K set, and limb-darkening values for the V passband were updated when changes in temperature and log g were produced, as with all light-curve modeling runs. Light-curve scatter is greater in this data set than in the others, because of larger intrinsic uncertainty, and possibly also because of the slightly larger range of the dates of the K data compared with the Wachmann data.

Three sets of models were produced as in the DW35 and W36 modeling. As for the W36 modeling, model 3 trials included both adjusted and fixed values. The model runs were characterized by

Model 1.—$T_1 > T_2, L_1 > L_2, q < 1$.

Model 2.—$T_1 < T_2, L_1 > L_2, q > 1$, T_2 fixed.

Model 3.—$T_1 > T_2, L_1 < L_2, q > 1$, T_2 adjusted.

The most consistent results were achieved for Model 3. All K data set modeling results are summarized in Table 8.

None of the models are able to fit the data particularly well because of the high intrinsic scatter, and the light curves appear little different from each other. The bottom panel of Figure 3 shows the fitting of a model with fixed T_2 and with additional weighting applied to values in the minima. The difficulty in fitting these data, which include two very low level values at secondary minimum, is obvious.

3.2.4. *General Comments*

For all three sets of light curve data, the parameter uncertainties for all runs involving adjustment of both stars' tem-

peratures are determined from runs where all but the quantities $\Delta\phi$, $T_{1,2}$, and l_3 were determined from final runs with $\Delta\phi$, l_3, and one of the temperatures unadjusted. The uncertainties for $\Delta\phi$ and l_3 values are from the prior runs with all 10 parameters adjusted. Where T_1 and i were not adjusted (the case for some model 2 and all model 3 runs), all uncertainties of parameters and model sets are from the single full set. The 300 K uncertainty for T_1 is an estimate based on the uncertainties of spectral type and temperature scale but is compatible with experiments in which T_1 was adjusted in, for example, the W36 set; the slightly higher uncertainty in T_2 derives from the error of the temperature difference (runs where T_1 was not adjusted) and that assumed in T_1. The relative uncertainty in ΔT as determined from the adjustment of T_1 in DW35 analyses (from trials when T_2 was not adjusted) was 42.8 K.

For the computation of absolute parameters, computed alone for the DW35 final model, the assumed color excess, $E_{B-V} = 0.16$, is taken from Twarog et al. (1997) and is a mean of those found for red giant and main-sequence stars. Adopting their selectivity ratio, $R = 3.1$, we obtain $A_V = 0.50$, and thus $A_B = 0.66$. The observed color index for the SS Lac system is $B-V = 0.162$, so the systemic intrinsic color index is found to be $(B-V)_0 \approx +0.00$. Solar values and spline-interpolated values for the bolometric corrections are derived from tabular data in Popper (1980).

4. DISCUSSION AND CONCLUSIONS

The radial velocity modeling confirms the analysis of Tomasella & Munari (1998) in all important details (see col. [4] of Table 4) and clearly establishes the mass ratio of the system, the orbital eccentricity, the systemic velocity, and the argument of periastron, within errors. The RV-based results therefore appear to be reliable.

4.1. *Determination of System Properties*

Whenever solutions for the DW35 set were obtained, the parameters of the converged solution were inserted in the input file of the TM98 data set and the RV modeling was redone. Iterations were carried out until mutually consistent results were obtained. The RV results for the adopted model are seen in column (3) of Table 4; they are thus consistent with the photometric solution of the best (if composite) light-curve set, DW35.

There is only a slight difference in parameters as revealed on the one hand by the modern RV data set and on the other by a photometric data set representing the average behavior of the system early in the 20th century. The iterated values of e and ω found for the final DW35 and TM98 data sets disagree, however. This may merely confirm that our single passband light curve is a composite of changing light-curve characteristics. In the W36 and K data sets, incomplete and high-scatter light curves preclude a precise comparison of all parameters. Taken together, the ω and $\Delta\phi$ values may reveal some evidence of apsidal motion, although, formally, any change in ω is hidden in the uncertainties. In any case, our solutions probably represent the best that can be uncovered until more data come to light or become available, or, of course, until the system begins to eclipse again.

The solutions to the three models for the DW35 data set give essentially the same Russell elements as obtained by Dugan & Wright (1935), but in model 3, the primary minimum is an occultation, in models 1 and 2, a transit. Dugan & Wright (1935) do not indicate which; they designate the larger star as 1 but do not indicate if this means the star eclipsed at primary minimum as in modern (Wilson-Devinney) usage. They assume uniform disks for the stars and equal surface brightnesses, the latter based on the apparent equality of depths of their mean light curve. Dugan & Wright (1935) found the relative luminosity of the larger component, which we designate by the subscript g (and the smaller component by s) to be $L_g/(L_g + L_s) = 0.68$; $r_g = 0.084a$, and $r_s = 0.057a$. They also indicate that to avoid having a negative value for $\cos^2 i$, they are forced to assume a central eclipse with $i = 90°$. For these quantities (we note that the larger star is our star 2, the nominally cooler component), we find that $L_g/(L_g + L_s) = 0.69$; $r_s = 0.0549 \pm 0.0003a$, and $r_g = 0.0838 \pm 0.0012a$. We also find no improvement in fitting the DW35 set for inclinations other than 90°. The similarity of the characteristics of the system across our models as well as the Russell model of Dugan & Wright (1935) indicates the basic derived properties to be surprisingly robust. If variations in the system over the 45 yr of data represented by this data set have not compromised the value of the light curve, therefore, the properties may be trustworthy. Within the errors, the parameters agree, with the exception of Ω_1 and L_1, which differ significantly between the photographic data sets' solutions and the visual K data set solution, and the phase shift required to make the computed light curve fit the observations. Some of the L_1 difference is attributable to the slight difference in the components' surface brightnesses between passbands, but not all of it. The derived absolute parameters based on the best-fit DW35 data set and on the radial velocity modeling are shown in Table 9.

The relative B magnitudes follow from the relative luminosity in the photographic region, taken for present purposes as the B passband. We can use these quantities in turn to compute the visual magnitudes of the components. From the Popper (1980) tabulated color indices appropriate to stars with the adopted T_1 and T_2 values, with $E_{BV} = 0.16$ and with $(B-V)_{1_0} = 0.06$, and $(B-V)_{2_0} = 0.09$ and $(B-V)_1 = 0.22$ and $(B-V)_2 = 0.25$ for stars 1 and 2, respectively. For this purpose, we ignore the solution for the Kordylewski data set because of the larger derived uncertainty in $L_1(V)$. From the relative luminosity and the apparent B system magnitude, we derive the apparent magnitudes of the components: $B_1 = 11.51 \pm 0.02$ and $B_2 = 10.67 \pm 0.01$. From our discussion of modern system magnitudes and color indices in § 2.1, $(B-V)_{1+2} = 0.162 \pm 0.003$ and $V_{1+2} = 10.097 \pm 0.003$, so that $B_{1+2} = 10.259 \pm 0.004$. Since $A_B = 0.66$, $B_{(1+2)_0} = 9.60 \pm 0.01$, $B_{1_0} = 11.51 \pm 0.02$, and $B_{2_0} = 10.67 \pm 0.01$. The components' intrinsic color indices obtained from general temperature-color relations are found to be redder than the observed system color index corrected for reddening. If the former intrinsic color indices are adjusted by approximately -0.07 so that their weighted average is made to equal that actually observed for the system, then the predicted apparent $B-V$ quantities become $(B-V)_1^{\rm pred} = 0.14$ and $(B-V)_2^{\rm pred} = 0.17$. The predicted $V_{1,2}$ values, 11.37 ± 0.02 and 10.50 ± 0.02, follow. From them, $V_{1+2}^{\rm pred} = 10.09 \pm 0.030$ is obtained, in satisfactory agreement with the observed system magnitude. The location of the system and components on the color-magnitude diagram of NGC 7209 (adapted from Hoag et al. 1961) can be seen in Figure 4.

TABLE 9

SS LACERTAE ABSOLUTE PARAMETERS[a,b]

Parameter (Units)	Star 1	System	Star 2
a ($R_\odot$)	21.8 ± 1.0	(43.3 ± 0.8)	21.6 ± 0.6
e	...	0.111 ± 0.002 (0.122 ± 0.018)	...
ω (deg)	...	355 ± 11 (354 ± 9)	...
V_γ (km s^{-1})	...	(−19.9 ± 0.8)	...
q	...	(1.009 ± 0.035)	...
i[c] (deg)	...	90 ± ~5 (76.5 ± ~3)	...
M ($M_\odot$)	2.62 ± 0.16	5.25 ± 0.31	2.64 ± 0.19
T (K)	8750 ± 300	...	8542 ± 309
$\langle R \rangle$ ($R_\odot$)	2.38 ± 0.02	...	3.63 ± 0.07
L ($L_\odot$)	29.9 ± 4.1	...	63.3 ± 9.4
M_{bol} (mag)	+1.00 ± 0.15	−0.23 ± 0.22	+0.19 ± 0.16
M_V (mag)	+1.08 ± 0.16	−0.17 ± 0.23	+0.19 ± 0.17
V (mag)	11.37 ± 0.02	10.097 ± 0.003	10.50 ± 0.02
(log g) (cgs)	4.10 ± 0.03	...	3.74 ± 0.05
BC (mag)	−0.08	...	−0.06
A_V (mag)	...	0.50	...
$(V-M_V)_0$ (mag)	...	9.77 ± 0.23	...
r (pc)	...	898 ± 95	...

[a] From the adopted solutions from Wilson-Devinney analyses of the DW35 (or TM98) data set.

[b] The uncertainties in this table are mean standard errors (S. D. S.).

[c] The inclination varies with time; $i = 90°$ at ~1912; $i = 76.°5$ at ~1998.

4.2. *Investigation of the Amplitudes in the Remeasured Harvard Plate Data*

Since the modeling results depend in a major way on measurements from the Dugan & Wright plot, the reliability of the data was investigated in the following way. First, we examined the Schiller et al. (1996) remeasured Harvard plate material and determined that the accumulated individual-points light curve agreed with the mean light curve (as selected from the plot) in most significant ways within the scatter.

Next we looked at the time behavior of the data at minimum phase. Values from S. J. S.'s remeasured Harvard data from the interval 1890–1937 suggest that both minima are visible over those dates, but they are not equally represented throughout the whole range. Distribution of the minima may account for the mean light curve of Dugan & Wright (1935), which has equal and modest eclipse depths (~0.41). Among the remeasured HCO plates, there is only one pair of data from primary minimum after 1907, but secondary minimum data were recorded also from 1923, 1928, and 1937. These are single observations only, with large measurement error (~0.1 mag) and not precisely at mid-minimum, but the last two have an average depth of ~0.2 mag The mean eclipse depths of the remeasured Harvard plate data alone are for primary minimum (PM) of 0.322 ± 0.116(m.e.) at a mean epoch of $\langle$HJDN$\rangle$ = 2,415,417.3 = 1901.089, but this includes two very low and possibly anomalous points from 1906; and for secondary minimum (SM) of 0.378 ± 0.141(m.e.) at a mean epoch of $\langle$HJDN$\rangle$ = 2,417,348.6 = 1906.377. The averages are dominated by the values for the 1897 season, when both eclipses were well observed, 0.336 ± 0.125(m.e.), and 0.374 ± 0.143(m.e.) for PM and SM, respectively. But for 1902, the PM average is 0.536 ± 0.077(m.e.), based on three minima, while the SM depth in this year was ~0.41 ± 0.11. For the interval 1915–1930, there are only 39 plates in total, and only one SM value is represented. We conclude that there is no strong evidence for an intrinsic difference between the minima, but systematic variations within the error in the relative depths cannot be ruled out.

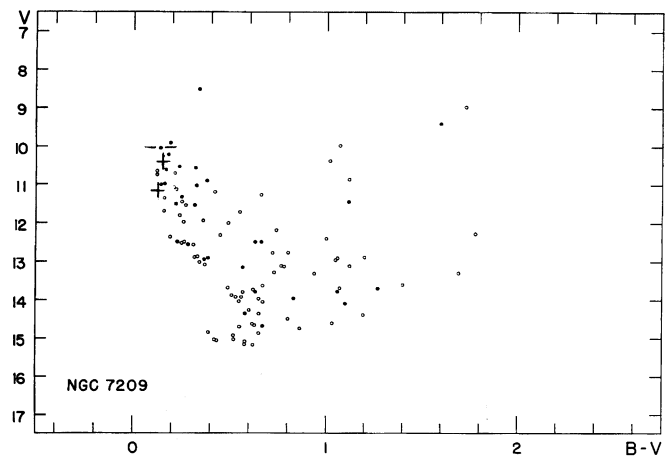

FIG. 4.—Color-magnitude diagram for NGC 7209 from Hoag et al. (1961), showing the relative locations of the SS Lac system and components from the analysis of the present paper.

As noted earlier, eclipse cessation can result from several causes: motion of the apsidal line; change in radius of one of the components; or variation of the observed orbital inclination because of nodal motion. The apsidal and nodal motions involve a third component, and careful studies by a number of investigators have revealed that the motion of the eclipsing binary orbit plane in a three-body system can account for light-curve amplitude variation. In particular, eclipse depth variation but not eclipse width variation has been seen in the eclipsing systems λ Tauri, β Persei, RW Persei, IU Aurigae, and AY Muscae.

Lehmann (1991) has argued that nodal motion is the cause of the variable amplitude of SS Lac. In an effort to check Lehmann's conclusions and to find the best date of the end of the eclipse era, we tabulated the amplitudes of all

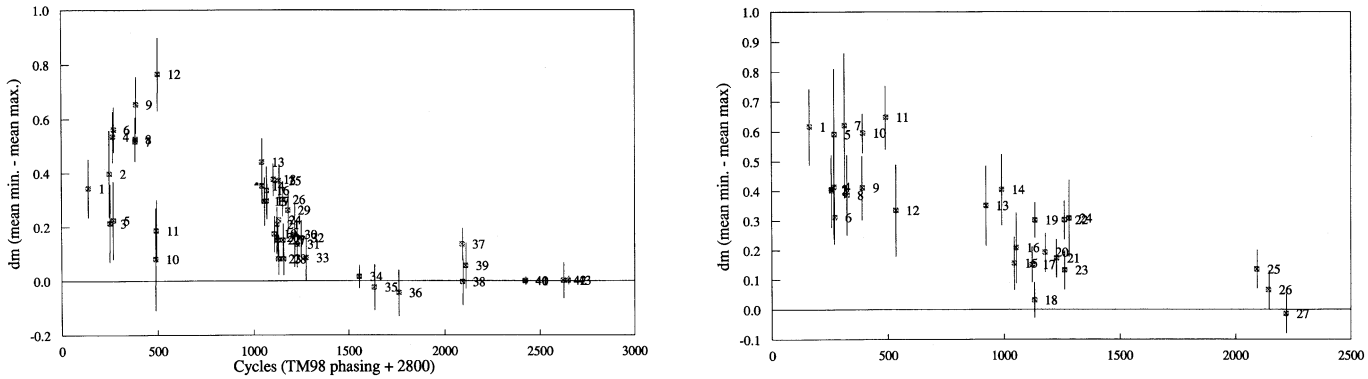

FIG. 5.—Amplitudes of the minima of historic SS Lac light curves as a function of cycle number for primary (*left*) and secondary minimum (*right*). The numbers refer to the first column line entries in Tables 10 and 11, respectively. "Amplitude" here means only the mean of low-light values observed within $\sim \pm 0.04^P$ of predicted minimum phase (with the elements of Tomasella & Munari 1998). The error bars are approximate mean standard errors only, deduced either from deviations about the mean of the low-light errors in that minimum or in the case of single observations, from the deviations about the mean of the maxima of the relevant data set.

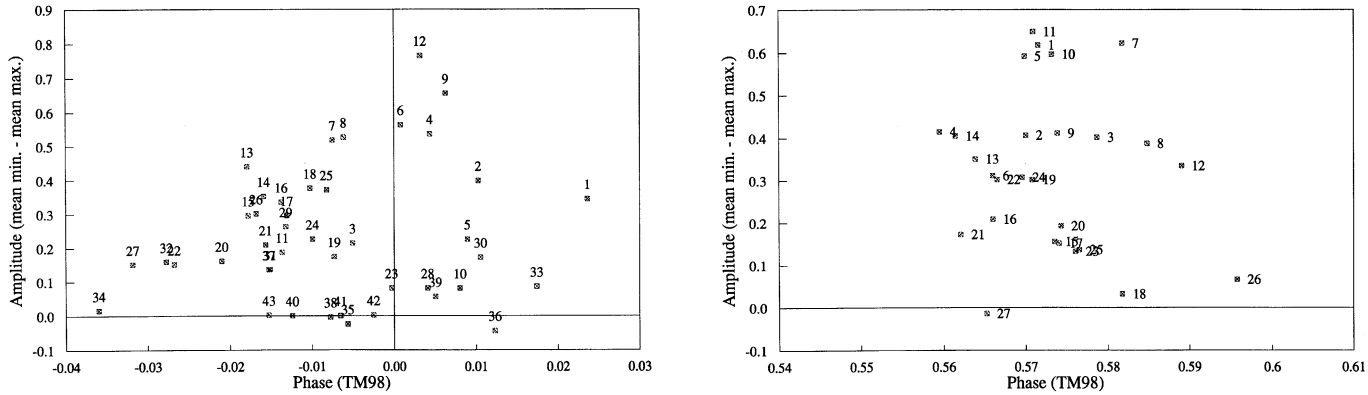

FIG. 6.—Distribution of the phase of the low-light level data plotted in Fig. 5. The numbers for the primary and secondary minimum plots refer to the first column line entries in Tables 10 and 11, respectively. Note that not all the lower amplitudes in earlier cycles can be explained by being from the branches of the minima.

data available to us. The remeasured Harvard plate data by Schiller et al. (1996), the visual estimates of Kordylewski et al. (1961), and the photographic data published by Wachmann (1936), Nekrasova (1938), and Mossakovskaya (1993) have been examined for all data in the vicinity of the minima according to the best ephemeris to date, that of Tomasella & Munari (1998). The values near the minima were averaged and compared to the mean light at maximum. Tables 10 and 11 and Figure 5 summarize these results. The uncertainties in the amplitudes are based on the mean standard errors of the averages; where only one low-light datum was available, the uncertainty for a single observation at maximum light was used. One might expect that some low values could well be on the branches, and thus underestimate the true eclipse depth, but Figure 6 demonstrates that this effect cannot be paramount since not all low-light values are greatly displaced from phases of predicted minimum light.

A parabolic fitting of the primary minimum low data points, seen in Figure 7, provides an approximate estimate of the date of mid-maximum (central) eclipse: 2,419,235.5 (AD 1911.5) and also provides the roots for the $y = 0$ condition, viz., the absence of eclipses: 2,409,663 (1885.3) for the onset and 2,428,807 (1937.75) for the termination. The interval of eclipse visibility, which by analogy with the lunar case, can be referred to as an *eclipse season*, would be 52.2 yr if this representation were accurate. Of course the eclipse amplitude curve is not expected to be a parabola, and many empirical curve fittings through the data are possible. Accordingly, a number of peak fitting curves were tried also. One of the functions that best fits the slopes on either side of the maximum (which is not actually seen in the available

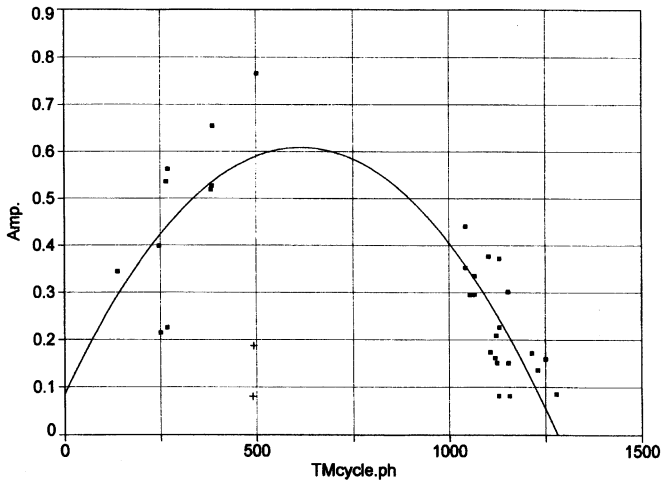

FIG. 7.—Fitting of a parabola to the depth of minima at phase zero as a function of cycle. The peak is found to occur at 1911.5; the intercepts, where eclipses cease, at 1885.3 and 1937.8.

TABLE 10

SS LACERTAE LIGHT-CURVE PRIMARY MINIMUM AMPLITUDE[a]

Source and Year	N_{obs}	HJD	Cycle Phase[b]	Amplitude[c]
1. Harvard 1892.70	1	2,412,354.673	139.024	0.345 ± 0.109
2. Harvard 1896.97	2	2,413,911.450	247.010	0.399 ± 0.160
3. Harvard 1897.08	1	2,413,954.478	249.995	0.215 ± 0.144
4. Harvard 1897.68	1	2,414,170.860	265.004	0.536 ± 0.094
5. Harvard 1897.76	3	2,414,199.759	267.009	0.226 ± 0.144
6. Harvard 1897.83	1	2,414,228.474	269.001	0.563 ± 0.083
7. Harvard 1902.33	2	2,415,871.822	382.993	0.519 ± 0.041
8. Harvard 1902.41	10	2,415,900.674	384.994	0.527 ± 0.081
9. Harvard 1902.49	1	2,415,929.686	387.006	0.655 ± 0.103
10. Harvard 1906.56	6	2,417,414.598	490.008	0.081 ± 0.189
11. Harvard 1906.67	1	2,417,457.535	492.986	0.187 ± 0.114
12. Harvard 1907.03	7	2,417,587.525	502.003	0.766 ± 0.133
13. Pagaczewski 1928.38	6	2,425,386.482	1042.982	0.440 ± 0.089
14. Kordylewski 1928.38	7	2,425,386.511	1042.984	0.352 ± 0.066
15. Pagaczewski 1928.86	7	2,425,559.481	1054.982	0.295 ± 0.089
16. Pagaczewski 1929.33	3	2,425,732.535	1066.986	0.335 ± 0.089
17. Kordylewski 1929.33	3	2,425,732.545	1066.987	0.296 ± 0.066
18. Wachmann 1930.75	2	2,426,251.576	1102.990	0.377 ± 0.060
19. Kordylewski 1930.91	14	2,426,309.284	1106.993	0.174 ± 0.066
20. Wachmann 1931.42	1	2,426,496.499	1119.979	0.162 ± 0.060
21. Kordylewski 1931.50	3	2,426,525.409	1121.984	0.209 ± 0.066
22. Wachmann 1931.62	1	2,426,568.498	1124.973	0.152 ± 0.060
23. Wachmann 1931.78	1	2,426,626.544	1129.000	0.082 ± 0.060
24. Kordylewski 1931.86	5	2,426,655.239	1130.990	0.226 ± 0.066
25. Wachmann 1931.86	1	2,426,655.264	1130.992	0.372 ± 0.060
26. Wachmann 1932.72	1	2,426,972.300	1152.983	0.302 ± 0.060
27. Wachmann 1932.76	1	2,426,986.500	1153.968	0.152 ± 0.060
28. Wachmann 1932.88	2	2,427,030.267	1157.004	0.082 ± 0.060
29. Harvard 1933.79	2	2,427,361.595	1179.987	0.263 ± 0.076
30. Nekrasova 1935.17	3	2,427,866.510	1215.010	0.172 ± 0.119
31. Mossakovskaya 1935.76	1	2,428,082.386	1229.985	0.136 ± 0.085
32. Kordylewski 1936.55	3	2,428,370.532	1249.972	0.159 ± 0.066
33. Mossakovskaya 1937.62	1	2,428,760.424	1277.017	0.086 ± 0.085
34. Mossakovskaya 1948.59	4	2,432,767.408	1554.964	0.016 ± 0.043
35. Mossakovskaya 1951.67	1	2,433,892.323	1632.994	−0.024 ± 0.085
36. Mossakovskaya 1956.68	1	2,435,723.462	1760.012	−0.044 ± 0.085
37. Mossakovskaya 1969.78	2	2,440,509.303	2091.985	0.136 ± 0.060
38. Mossakovskaya 1969.87	1	2,440,538.303	2093.992	−0.004 ± 0.085
39. Mossakovskaya 1970.54	1	2,440,783.507	2111.005	0.056 ± 0.085
40. RAO (V) 1982.81	1	2,445,266.750	2431.988	0.000 ± 0.015
41. RAO (V) 1982,89	1	2,445,295.667	2423.993	0.000 ± 0.015
42. RAO 1990.67	1	2,448,135.752	2620.997	0.002 ± 0.066
43. RAO 1991.73	7	2,448,524.810	2647.985	0.002 ± 0.017

[a] The uncertainties in this table are mean standard errors (S. D. S.).
[b] Phased as per Tomasella & Munari 1998, eq. (2).
[c] The difference between mean minimum and maximum values.

amplitude data) is the three-parameter error function peak,

$$y = a + b \text{ erfc } \{[(x - b)/c]^2\} ,$$

where the coefficients are determined to be the amplitude at maximum, $a = 0.694 \pm 0.063$; the cycle number at maximum, $b = 644.098 \pm 16.476$; and a width parameter, $c = 0.7240 \times \text{FWHM} = 574.2 \pm 38.1$ so that the FWHM $= 793.1 \pm 52.6$.

The b and c coefficients correspond to the calendar year 1912.64 ± 0.65 and width paraneter of 22.7 ± 1.5 yr, respectively. The $FWHM$ corresponds to 31.3 ± 2.1 yr, for an eclipse season of 62.6 yr. The point at which the function reaches 0 amplitude is $\approx$1946.4, but the amplitude changes slowly at amplitudes below 0.05, at $\sim$1937.8. Thus, in the absence of photoelectric data at this date, this effectively marked the end of observable eclipses. Other peak-fitting curves did not match the slopes as well, having too high or too extended flat maxima. The combined primary and secondary minima data were also fitted, with similar results but higher uncertainties.

As suggested by Lehmann (1991), the amplitude variation may, itself, be expected to resemble the minimum of an eclipsing light curve. We can expect symmetry from such a light curve, and there are many observations (of the amplitude vs. time/cycle number) near the end of the sequence and many just before the apparent peak that suggest such symmetry at least at the primary minimum. For component stars of equal brightness, the greatest depth to be expected is $\sim$0.75 during total eclipse. The existing data set shows no such depth and no evidence of a standstill, but neither can

TABLE 11

SS LACERTAE LIGHT-CURVE SECONDARY MINIMUM AMPLITUDE[a]

Source Year	N_{obs}	HJD	Cycle Phase	Amplitude[b]
1. Harvard 1893.59	1	2,412,679.733	161.572	0.618 ± 0.127
2. Harvard 1897.30	1	2,414,034.851	255.570	0.407 ± 0.107
3. Harvard 1897.38	2	2,414,063.808	257.579	0.402 ± 0.122
4. Harvard 1897.78	4	2,414,207.696	267.560	0.415 ± 0.175
5. Harvard 1897.86	1	2,414,236.678	269.570	0.592 ± 0.220
6. Harvard 1897.94	1	2,414,265.454	271.566	0.312 ± 0.090
7. Harvard 1899.63	1	2,414,885.586	314.582	0.622 ± 0.242
8. Harvard 1900.03	3	2,415,029.794	324.585	0.388 ± 0.134
9. Harvard 1902.67	2	2,415,995.534	391.574	0.411 ± 0.108
10. Mossakovskaya 1902.75	1	2,416,024.357	393.573	0.596 ± 0.065
11. Harvard 1906.66	1	2,417,451.546	492.571	0.649 ± 0.106
12. Harvard 1908.36	1	2,418,071.711	535.589	0.335 ± 0.155
13. Harvard 1923.55	1	2,423,621.654	920.564	0.351 ± 0.134
14. Nekrasova 1926.27	1	2,424,616.350	989.562	0.405 ± 0.120
15. Pagaczewski 1928.45	1	2,425,409.425	1044.574	0.155 ± 0.089
16. Harvard 1928.76	1	2,425,524.647	1052.566	0.209 ± 0.119
17. Wachmann 1931.48	1	2,426,519.494	1121.574	0.152 ± 0.059
18. Wachmann 1931.84	1	2,426,649.352	1130.582	0.032 ± 0.059
19. Wachmann 1931.96	1	2,426,692.444	1133.571	0.302 ± 0.059
20. Kordylewski 1933.66	2	2,427,312.399	1176.574	0.192 ± 0.065
21. Kordylewski 1935.67	1	2,428,047.458	1227.562	0.172 ± 0.065
22. Kordylewski 1936.97	4	2,428,523.262	1260.567	0.302 ± 0.065
23. Kordylewski 1937.05	1	2,428,552.232	1262.576	0.132 ± 0.065
24. Harvard 1937.76	1	2,428,811.634	1280.570	0.308 ± 0.130
25. Mossakovskaya 1969.77	1	2,440,503.418	2091.577	0.136 ± 0.065
26. Mossakovskaya 1971.75	1	2,441,224.514	2141.596	0.066 ± 0.065
27. Mossakovskaya 1974.70	1	2,442,305.302	2216.565	−0.014 ± 0.065

[a] The uncertainties in this table are mean standard errors (S. D. S.).
[b] The difference between mean minimum and maximum values.

be ruled out because of gaps in the data. Confirmed observation of any minima outside the dates of extrapolated zero would be interesting, since they are unexpected, and so would data in the gap when the amplitude should have been at maximum.

The Ischenko estimates of the Tashkent plates referred to in § 2.1 are presented on time and phase axes in Figure 8. They support rather dramatically the evidence for an effective absence of eclipses in about ~1937 and further question the credibility of the Tashpulatov (1965) light curve. Since the data set of Nekrasova (1938), though sparse, and the extensive compilations of Mossakovskaya (1993) point to the same conclusion, this essentially clinches the matter. The overall results confirm the conclusion of Lehmann (1991) of an apparent decrease in amplitude in the 1920s and 1930s, and we confirm that the apparent maximum in the amplitude seems to have been reached in the early years of this century, in about 1911.

The light-curve results are sufficiently uncertain that variations in certain other parameters, such as the radius of one of the stars, cannot be ruled out. The formal solutions indicate a larger difference in monochromatic luminosity

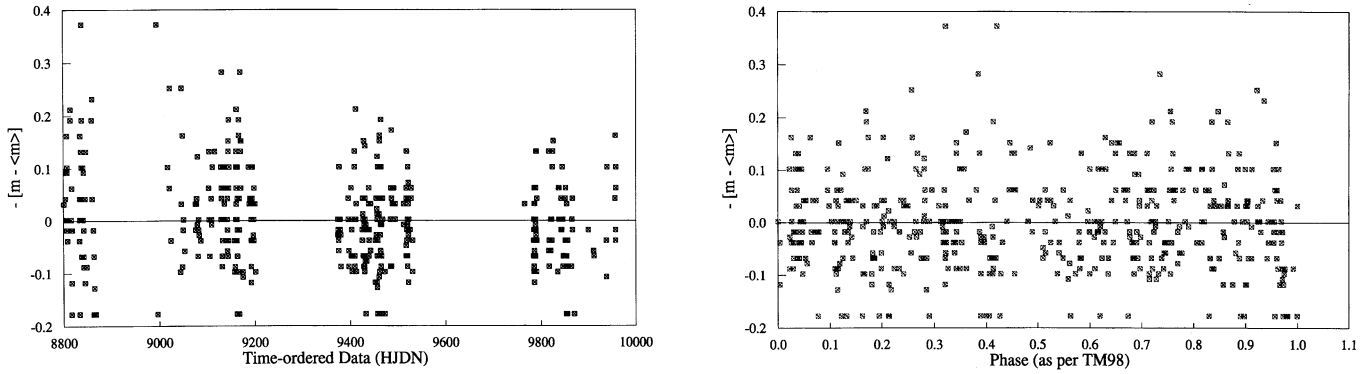

FIG. 8.—Light curve of SS Lacertae based on more recent estimates from Tashkent plates taken between 1937 and 1940 by I. M. Ischenko and by M. Zakirov (1998, private communication). The magnitude estimates were averaged and the differences between the individual values taken to produce the plots. *Left*, The time-sequence behavior of the data; *right*, the phased data, produced with the elements of Tomasella & Munari (1998). Together with Fig. 7, these plots support the suggestion of Mossakovskaya (1993) that eclipses ceased between 1937 and 1940.

(2×) between the components than does the present spectral study, which indicates the more massive star (star 2) to be slightly more luminous (Tomasella & Munari 1998). It is more likely, however, that evidence of variation from differing parameters for different light-curve sets arises from light-curve anomalies introduced by the apparent variable depth of eclipses.

We have noted that the Dugan & Wright (1935) mean light curve is a composite of variable light curves, especially in the area of the secondary minimum. The main effect of this variation seems to be a larger scatter in the depth of the secondary minimum than is seen in the primary minimum. The scatter in the Kordylewski data, which are quite numerous and consistent in the maximum, with $\sigma_1 = \pm 0.065$, is larger in the minima, especially the secondary minimum, even though the mean depth does not exceed ~ 0.3 mag. However, the explanation may lie in a remark by Hoffmeister (1921) that he, at least, found it difficult to estimate the brightness of SS Lac because of its small light variation and the rich numbers of stars of nearly equal brightness in the star cluster.

The minima from the 1930s show amplitudes ~ 0.4 mag, in agreement with the amplitude in the HCO data from ~ 1900. The detailed plots of the cycle-to-cycle amplitudes reveal apparent variation in both minima. Figure 5 shows that the variation of the inclination over the data sets causes a cycle-to-cycle change in the amplitude of the system; the averaging of data sets over several years results in an average minimum depth that is not greatly different in the two principal sets we analyze here.

To categorize the behavior of the system, a series of experiments was performed with the Binary Maker 2.0 software of Bradstreet (1993), which, although unsuited to fully explore eccentric orbit cases, provides an indication of how this is possible. The experiments demonstrate that total eclipses for the DW35 fitting model occur for all inclinations greater than $\sim 88\overset{\circ}{.}1$, while the depths of the eclipses decrease slowly for decreases in i to about $\sim 87\overset{\circ}{.}5$. The decrease is more rapid thereafter until the cessation of eclipses altogether at $i = \sim 82°$. The BM2.0 experiments coupled with the parabolic fit of the individual cycle amplitudes suggest that the total range of inclination variation over a 26 yr interval is about 8°. If the motion were purely secular and uniform, the period of revolution of the orbital plane would be ~ 1200 yr, in agreement with that found by Tomasella & Munari (1998), 1275 ± 90 yr. A slight refinement is found by making use of the derived values of the inclination for the modeled data sets (see Fig. 9). Since it is iterated with the DW35 set, the TM98 point is neither independent nor a mere extrapolation, but lies along a line satisfied, within errors, by the other points.

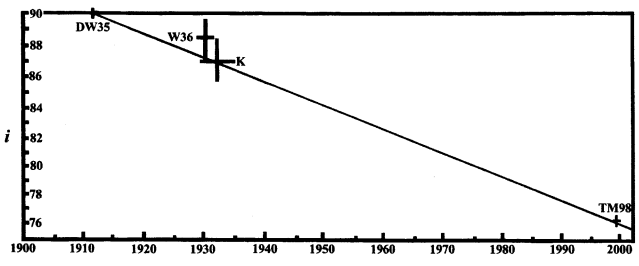

FIG. 9.—Derived inclinations from the final models of all analyzed data sets, and the limit from eclipse cessation simulations. The 90° inclination placement at the year 1912 is derived from the Harvard plates light curve amplitude study begun by S. J. S.; that at 1997 is due to the iterated solution for the TM98 data set; that at 82° is the epoch of eclipse cessation.

We noted in § 3.2 that an optimum value for $i = 76\overset{\circ}{.}5$ was obtained. If this is accurate, we have over the 1998–1912 span of years a change of $13\overset{\circ}{.}5$ for a variation of $\approx 0\overset{\circ}{.}157$ yr^{-1}, for a period of ~ 2300 yr or an interval between eclipses of length ~ 1150 yr (if the orbital motion of the SS Lac system permits eclipses to be seen at both nodes).

Within errors, Tables 6, 7, and 8 suggest no discernible apsidal motion to be present in the system, in agreement with statements by Dugan & Wright (1935), Dugan & Wright (1937), and Shapley & Swope (1938).

Regrettably, the data in hand for individual observations of the minima in the early HCO data are too sparse and noisy for short-interval light-curve precision modeling at present, which could confirm the amplitude and parameter variation predictions over short intervals. It would be of great value to have available the full set of Hoffmeister's (1921) estimates, which cover only a narrow range of dates, the full set of Harvard estimates, and the full archival set of Sonneberg data. According to T. Lehmann (1993, private communication), efforts were underway, at one point, to measure these plates. S. J. S. plans further work in this area to improve our knowledge of the behavior of this system, especially around the predicted date of maximum eclipse, 1912.

In any case, the system has certainly not been disrupted as had sometimes been conjectured. The strongest evidence for this scenario was a CCF analysis (Schller & Milone 1996) in which the hydrogen lines were excluded (see § 2.2). A reexamination of the intensified Reticon spectral registration shows broad and noisy cores in the Balmer lines and, although sometimes suggestive, no firm evidence of splitting. Apparently, the S/N in these spectra was insufficiently high to reveal the SB2 character of the system.

Regarding the third component, it is interesting to note that the mean radial velocity from 12 exposures found by S. J. S., -24.9 ± 4.8 km s^{-1}, is in agreement with the third component radial velocity seen at quadratures by Tomasella & Munari 1998 (-22.3 ± 3.0) and that these values are not significantly different from the Tomasella & Munari mean radial velocity determination (-21.2 ± 0.3), from that derived here (-19.9 ± 0.8), or from the mean velocity of three giants in NGC 7209 measured by J.-P. Mermilliod (1995, private communication to S. J. S.; -19.1 ± 0.2).

We note that the derived distance for the system (Table 9), 898 ± 95 pc, $(V_0 - M_V) = 9.77 \pm 0.23$, is in approximate agreement with that found for SS Lac in the Vilnius photometry study of NGC 7209 by Vansevičius et al. (1997), 1040 ± 10 pc, computed on the basis of equal luminosity for the components. This value is also close to their value for the cluster distance, 1026 ± 15, corresponding to a corrected distance modulus of 10.06 ± 0.06. Their derived V magnitude of the SS Lac system (their star 1828) is 10.07. Our result is not, however, consistent with that of Peña & Peniche (1994), who find a distance for SS Lac (their star 16) of only 634 pc and place it in the closer of what they argue are two superposed clusters. Because Vansevičius et al. (1997) closely scrutinized the stars they included for membership, we accept their determination for the cluster distance (if not their distance for SS Lac, since our solutions suggest disparate luminosities) and thus the unitary quality of the cluster.

Therefore, on the grounds of proximity on the sky, proper motion, radial velocity, photometry, and derived properties, the binary is confirmed as belonging to NGC 7209. Moreover, on the basis of its apparent connection to the binary, and radial velocity agreement with it, the third component seen at quadratures by Tomasella & Munari (1998) in the spectra is a probable cluster member, as well as the likely source of the binary's nodal motion.

The studies of Söderhjelm (1974, 1975) of the behavior of the triple systems β Per, AY Mus, and λ Tau suggest that nodal variation may be accompanied by apsidal motion and characterized by variable separation and widths of the eclipses. Thus far, at least, no certain evidence is seen for these effects in SS Lac.

An upper limit to the angular separation of the third component from the close binary, either through *Hubble Space Telescope* or ground-based adaptive optics, would be useful. It would also be useful to obtain high-resolution radial velocities, from which the period of the mutual orbit of the close binary and the third component could be found. The results of current modeling suggest that the contribution from a third light source could be hidden in the noise in the photographic light curves and in almost all of the K data set modeling. In the W36 model 3, l_3 exceeds its error, but only marginally. In the K model 3 of Table 8, l_3 is significantly greater than its uncertainty, but in that model, $l_3 \approx 27\%$. The noise level sets the limit $l_3 \lesssim 2\%$ in the DW35 data set modeling. Given the relative dimness of the third star's contribution to B and its weak detection in the Balmer α, β, and γ lines, one would suppose it to be both less luminous and more red than the other components. A study in the infrared is underway at the *RAO* to check this possibility.

The curious circumstance that the components essentially agree in mass and in temperature and yet differ significantly in radius is enigmatic, if the solutions presented here are to be believed. Unfortunately, there seems little chance to improve on the solutions until more archival data come to light or the system begins to eclipse again. It is instructive, however, that the initial Russell solution of Dugan & Wright as well as each of the photometric sets we analyzed in the present work yields disparate values for the eclipsing components' luminosities and sizes. The location of the SS Lac components on the blue side of the CMD, and just below the cluster turn-off, continues to make this system important as a check on stellar evolution models; perhaps astronomers of the fourth (or fifth!) millenium may also find it so.

We are grateful for several grants that have supported this work: Support to E. F. M. has come from the University of Calgary Research Grants Committee and from NSERC of Canada; research support to S. J. S. has been provided by a Northwest Area Foundation Grant of the Research Corporation, the NASA SDSU JOVE program, a NASA grant administered by the American Astronomical Society, NSF grant OSR 94-52894 and by the South Dakota Future Fund. Steven Griffin, James van Leeuwen, Jason McVean, and Perry Radau helped in the acquisition of the photoelectric data summarized in Table 1. David Fry and Eric Leblanc provided important copies of critical references from DAO's library. A special word of gratitude should be voiced for the careful work of the Cracow observers, and to Rosa Szafraniecz, who enabled these valuable data to come to light. See Milone et al. (1980) for their contributions to the study of another interesting variable, RW Com. This research has made use of the SIMBAD database, operated at CDS, Strasbourg, France.

REFERENCES

Artiukhina, N. M. 1961, Trudy. Astron. Inst. Sternberg, 30, 196
Bradstreet, D. H. 1993, Binary Maker 2.0 User Manual (Norristown, PA: Contact Software)
Dugan, R. S., & Wright, F. W. 1935, AJ, 44, 150
———. 1937, AJ, 46, 148
Etzel, P. B., & Vogelnau, N. H. 1996, IAU Circ. 6344
Etzel, P. B., Vogelnau, N. H., & Nguyen, Q. T. 1996, IAU Circ. 6429
Harries, T. J., Hilditch, R. W., & Hill, G. 1998, MNRAS, 295, 386
Hill, G. 1982, Publ. Dom. Astrophys. Obs. Victoria, 16, 59
Hill, G., Fisher, W. A., & Poeckert, R. 1982, Publ. Dom. Astrophys. Obs. Victoria, 16, 43
Hoag, A. A., Johnson, H. L., Iriarte, B., Mitchell, R. I., Hallam, K. L., & Sharpless, S. 1961, Publ. US Naval Obs., 17, 347
Hoffmeister, C. 1921, Astron. Nachr., 214, 7
Kallrath, J. 1993, in Light Curve Modeling of Eclipsing Binary Stars, ed. E. F. Milone (New York: Springer), 39
Kallrath, J., & Milone, E. F. 1999, Eclipsing Binary Stars: Modeling and Analysis (New York: Springer)
Kallrath, J., Milone, E. F., Terrell, D., & Young, A. T. 1998, ApJ, 508, 308
Kordylewski, K., Pagaczewski, J., & Szafraniec, R. 1961, Acta Astron. Suppl., 4, 487
Kurucz, R. L. 1993, in Light Curve Modeling of Eclipsing Binary Stars, ed. E. F. Milone (New York: Springer), 93
Lacy, C. 1992, AJ, 104, 801
Lavdovska, V. V. 1962, Izv. Pulkovo Obs., 24, 69
Lehmann, T. 1991, Inf. Bull. Variable Stars 3610
Milone, E. F., Chia, T. T., Castle, K. G., Robb, R. M., & Merrill, J. E. 1980, ApJS, 43, 339
Milone, E. F., & Robb, R. M. 1983, PASP, 95, 666
Milone, E. F., Robb, R. M., Babott, F. M., & Hansen, C. H. 1982, Appl. Opt., 21, 2992
Milone, E. F., & Schiller, S. J. 1998, BAAS, 30, 1155
Milone, E. F., Stagg, C. R., & Kurucz, R. L. 1992a, ApJS, 79, 123
Milone, E. F., Stagg, C. R., & Schiller, S. J. 1992b, in Evolutionary Processes in Interacting Binary Stars, ed. Y. Kondo, R. F. Sistero, & R. S. Polidan (Dordrecht: Kluwer), 479
Mossakovskaya, L. V. 1993, Astron. Lett., 19, 35
Nekrasova, S. 1938, Perem. Zvezdy, 5, 182
Peña, J. H., & Peniche, R. 1994, Rev. Mexicana Astron. Astrofis., 28, 139
Pickering, E. C. 1907, Harvard Circ. 130
Platais, I. 1991, A&AS, 87, 577
Popper, D. M. 1980, ARA&A, 18, 115
Sandberg Lacy, C. H., Helt, B. E., & Vaz, L. P. R. 1999, AJ, 117, 541
Schaefer, B. E. 1981, PASP, 93, 225
Schaefer, B. E., & Fried, R. E. 1991, AJ, 101, 208
Schiller, S. J., & Milone, E. F. 1987, AJ, 93, 1471
Schiller, S. J., Bridges, D., & Clifton, T. 1996, in ASP Conf. Proc. 90, The Origins, Evolution, and Destinies of Binary Stars in Clusters, ed. E. F. Milone & J.-C. Mermilliod (San Francisco: ASP), 141
———. 1996, in ASP Conf. Proc. 90, The Origins, Evolution, and Destinies of Binary Stars in Clusters, ed. E. F. Milone & J.-C. Mermilliod (San Francisco: ASP), 120
Schiller, S. J., Milone, E. F., Zakirov, M. M., & Azimov, A. A. 1991, BAAS, 23, 879
Shapley, H., & Swope, H. H. 1938, Hvar Obs. Bull., 909, 5
Söderhjelm, S. 1974, Inf. Bull. Variable Stars 855
Söderhjelm, S. 1975, A&A, 42, 229
Stagg, C. R., & Milone, E. F. 1993, Light Curve Modeling of Eclipsing Binary Stars, ed. E. F. Milone (New York: Springer), 75
Stefanik, R. P., Torres, G., Caruso, J. R., & Davis, R. J. 1996, IAU Circ. 6433
Svolopoulos, S. 1961, ApJ, 134, 612
Tashpulatov, N. 1965, Perem. Zvezdy, 15, 424
Tomasella, L., & Munari, U. 1998, A&A, 335, 561
Twarog, B. A., Ashman, K. M., & Anthony-Twarog, B. J. 1997, AJ, 114, 2556

van Schewick, H. 1966, Veröff. Astron. Inst. Univ. Bonn, 70, 1
Vansevičius, V., Platais, I., Paupers, O., & Ābolinš, Ē. 1997, MNRAS, 285, 871
Wachmann, A. A. 1935, Astron. Nachr., 255, 340
Wachmann, A. A. 1936, Astron. Nachr., 258, 361
Wilson, R. E. 1963, General Catalog of Radial Velocties (Carnegie Publ. 601) (Washington: Carnegie Inst.)
———. 1992, Documentation of Eclipsing Binary Star Model (Gainesville: Univ. Florida)
Zakirov, M. M., & Azimov, A. A. 1990, Inf. Bull. Variable Stars 3487